UNIVERSITY OF CALIFORNIA, SAN DIEGO

Assessing seasonal primary production in Andvord Bay, Antarctica

A Thesis submitted in partial satisfaction of the requirements for the degree Master of Science

in

Oceanography

by

Lindsey Ekern

Committee in charge:

Katherine Barbeau, Co-Chair
Maria Vernet, Co-Chair
Teresa Chereskin

2017

The Thesis of Lindsey Ekern is approved and it is acceptable in quality and form for publication on microfilm and electronically:

Co-Chair

Co-Chair

University of California, San Diego

2017

TABLE OF CONTENTS

LIST OF FIGURES

LIST OF TABLES

ACKNOWLEDGEMENTS

I would like to acknowledge and thank my committee members Maria Vernet, Kathy Barbeau, and Teri Chereskin for their support and advise; my FjordEco and team Phyto co-conspirators: B. Jack Pan, Kiefer Forsch, Lauren Manck, Lars Thoresen, Angela Klemmedson, and Diane Gutierrez, the University of Hawaii at Manoa and University of Alaska at Fairbanks crews for enabling this project to be successful; and my family and friends for always being there when I needed them particularly Mattias Cape, Kim Null, Jamie Ekern, Jax Pan, and Indiana without whom this could and would not have been completed. I would like to especially thank Maria for the endless support and wonderful opportunity to embark on this adventure.

This research was supported by the US National Science Foundation, Office of Polar Programs, grant number PLR-1443705.

This thesis in part is currently being prepared for submission for publication of the material. Ekern, Lindsey; Pan, Boyang; Cape, Mattias; Vernet, Maria. The thesis author was the primary investigator and author of this material.

ABSTRACT OF THE THESIS

Assessing seasonal primary production in Andvord Bay, Antarctica

by

Lindsey Ekern

Master of Science in Oceanography

University of California, San Diego, 2017

Katherine Barbeau, Co-Chair
Maria Vernet, Co-Chair

The western Antarctic Peninsula is rapidly warming and its high-latitude fjord ecosystems are expected to be highly sensitive to climate warming (Weslawski *et al.* 2011; Cook *et al.* 2016). As the region continues to change, understanding the current nutrient budget will allow for better predictions of ecosystem response at all levels of the food web to variable future conditions. Analysis from two synoptic transects

along Andvord Bay, bracketing the 2015-2016 austral summer, allows for primary production to be assessed through the depletion of dissolved inorganic nutrients, nitrate and silicate. Andvord Bay is a quiescent system that can experience surface nutrient replenishment during katabatic wind events otherwise sustaining favorable growth conditions throughout an extended growth season. The high concentration of surface nitrate and minimal presence of reduced nitrogen species in spring suggests new production dominates the early season while an observed four-fold increase in ammonium would support late season recycled production. Silicate depletion indicates 25-68% of the primary production in Andvord Bay was from diatom growth from December 2015 to April 2016. Modifications were made to the nutrient drawdown method for primary production estimation to adapt to conditions unique to the Andvord Bay region, replacing the baseline winter water requirement and adapting the growth periods. Applied, this method yields reasonable, conservative estimates for net community new production indicating greater production inside the fjord than the outside waters of the Gerlache Strait and supporting the hypotheses that fjords in the WAP are hot-spots of productivity.

INTRODUCTION

The Southern Ocean (SO) is the largest high nutrient-low chlorophyll (HNLC) region of the world's ocean. The low phytoplankton biomass as gauged by chlorophyll-*a* (chl-a), despite the presence of excess surface macronutrients including nitrate (NO_3^-), phosphate (PO_4^{3-}), and silicate (SiO_4^{2-}), is thought to be controlled by grazing pressure and iron (Fe) limitation (Pitchford and Brindley 1999). There are, however, local areas of increased phytoplankton production within the SO, including along ice edges (Wilson *et al.* 1986), polynyas (Cape *et al.* 2014, Arrigo *et al.* 2015), fronts (Labscher *et al.* 1993) and in the western Antarctic Peninsula (wAP) shelf (Vernet *et al.* 2008), that correspond with rich biodiversity in the benthos (Smith *et al.* 2008). Andvord Bay has been suggested as one of these hotspots of phytoplankton primary production and biodiversity, serving as a feeding ground for krill and baleen whales (Nowacek *et al.* 2011), as well as demonstrating a diverse and abundant benthic community (Grange and Smith 2013). Understanding how much energy is harnessed through primary production and subsequently available for the ecosystem is particularly important when keystone species are present and is fundamental to predicting how ecosystems and biodiversity will respond to climate change (Robbins *et al.* 2011, Malcolm *et al.* 2006). The wAP is rapidly warming (Cook *et al.* 2005, 2016, Steig *et al.* 2009, Trivelpiece *et al.* 2011) and its high-latitude fjord ecosystems are expected to be highly sensitive to climate warming (Weslawski *et al.* 2011).

Phytoplankton, particularly diatoms, play an important role in the carbon cycle (Smetacek 1999). By fixing inorganic carbon (C), phytoplankton provide organic C for the food web as well as export to the deep ocean and sediments. When in place,

the short food chain of diatoms to krill to marine mammals illustrates incredible efficiency and implies a large phytoplankton biomass available for nutrient cycling and transport to the benthic community and sediments (Hart 1934). All phytoplankton require nitrogen (N), phosphorus (P) and Fe to grow; diatoms also require silicon (Si). Upwelling of the upper circumpolar deep water (UCDW) onto the wAP shelf delivers these macronutrients needed for phytoplankton growth (Martinson *et al.* 2008), while local glaciers could provide sufficient Fe (Annett *et al.* 2015) for primary production, as observed for ice shelves (Gerringa *et al.* 2012). The ratios of these elements in the water column can indicate growth limitation, identify dominant groups in the community, allow comparison of marine environments, and inform on nitrogen remineralization and Fe limitation (Kim *et al.* 2016). For example, typically, lower Si to N ratios in seawater indicates Fe replete growth conditions as phytoplankton increase Si uptake during Fe limitation (Takeda 1998). Additionally, diatoms preference for NO_3^- as a nitrogen source —even though it is more energy expensive to utilize than ammonium (NH_4^+)— (Lomas and Glibert 1999a,b), uniquely influences water column nutrient ratios when they bloom.

Primary production can be determined by ^{14}C uptake incubations and the analysis of stable C or oxygen isotopes (Marra 2002), and by remotely sensed ocean color data sets (Behrenfeld and Falkowski 1997). The accuracy of estimating net, and some gross, primary production using those methods depends on the specific variables utilized, such as incubation time. Another method to estimate primary production is based on nutrient drawdown. This latter method is based on four assumptions: (1) quantitatively compatible data sets if multiple cruises or multiple years are available;

(2) little or no vertical or lateral mixing; (3) known period of depletion since previous winter; and (4) known late-winter nutrient concentrations, including vertical homogeneity below sea ice (Jennings *et al.* 1984). Several relatively recent studies have used nutrient drawdown to estimate primary production: in the Pacific sector of the SO (Rubin *et al.* 1998), in the Weddell Sea (Jennings 1984, Hoppema *et al.* 2000), in the Arctic (Tremblay 2008, Bergeron and Tremblay 2014), in the Antarctic Peninsula (Priddle 1998), and in the Ross Sea (Arrigo *et al.* 2000, Long *et al.* 2011). Per Hoppema *et al.* (2000), who applied nutrient drawdown in the Weddell Sea, "the calculated depletions represent the time-integrated changes of the entire surface layer since the end of the winter period". Using this method, Jennings *et al.* (1984) concluded that the primary production in the Weddell Sea could be 2.5 times higher than previously thought.

The nutrient drawdown methodology utilized in these previously published studies, however, cannot be directly applied to wAP's glacio-marine fjords such as Andvord Bay. First, the fjords by definition have distinct geomorphology, circulation processes, and terrigenous inputs including glacial ice, meltwater, and sediments. Second, the fjords exhibit substantially different ecosystem forcing than their adjacent continental shelves or the open ocean. Third, for Andvord Bay there is no data set to span the length of a growth season. Utilizing the ^{14}C incubation method is also problematic for studying Andvord Bay because it is only possible to estimate daily productivity measurements during field campaigns. Such measurements are unlikely to be representative of a full growth season given the complexity expected in the region, including wind events and short, intense summer blooms (Jennings *et al.*

1984). Therefore, a full season estimate of primary production, as utilizing nutrient drawdown, may be more representative of C available to the rich benthic community (Grange and Smith), where high levels of diversity and activity require high phytodetrital and fecal fluxes to the seafloor.

These characteristics and challenges found in Andvord Bay make it a novel and attractive region in which to estimate primary productivity from nutrient drawdown. The Fe-replete coastal waters of the wAP (Ardelan *et al.* 2010) also provide an interesting regime to study phytoplankton growth and macro-nutrient cycling without the constraints, particularly micro-nutrient limitation, found in most open ocean ecosystems of the SO. As the wAP climate continues to change (Cook *et al.* 2005, 2016), understanding the current nutrient budget will allow for better predictions of the response of the ecosystem at all levels of the food web to variable future conditions.

METHODS

Cruises, Sampling and Analysis Protocols:

Hydrographic sampling was conducted on three National Science Foundation (NSF)-funded FjordEco Project cruises to the wAP: LMG15-10 (18 November to 28 December 2015 on ARSV Laurence M. Gould), NBP16-03 (30 March to 30 April 2016 on RVIB Nathaniel B. Palmer), and LMG17-02 (14 February to 21 March 2017 on ARSV Laurence M. Gould). The primary mission of LMG17-02 was to recover deployed sensors; as such FjordEco sampling during this cruise was limited to 26 February and 3-9 March 2017. Sampling on all three cruises was focused in and around Andvord Bay, approximately 64.8 °S, 62.6°W (Figure 1). The fjord is nearly 16 km long and 5 km in width from the inner fork to the entrance of the Aguirre and Errera Channels. The mouth widens, doubling its width, and opens to the Gerlache Strait approximately 25 km from the inner fork. The inner fjord is split with the dominant Bagshawe Glacier entering Lester Cove on the south and the Moser Glacier entering Henryk Cove in the northern branch. For the purpose of this paper, Andvord Bay will be will be described as the fjord (0-18 km from the glacier) with the inner-fjord (0-8 km along transect), the fjord mouth or outer-fjord (18-28 km along transect), and the Gerlache Strait (30-45 km along transect). Similar transects were sampled in December 2015 and April 2016 between Lester Cove and Henryk Cove, respectively, and the Gerlache Strait.

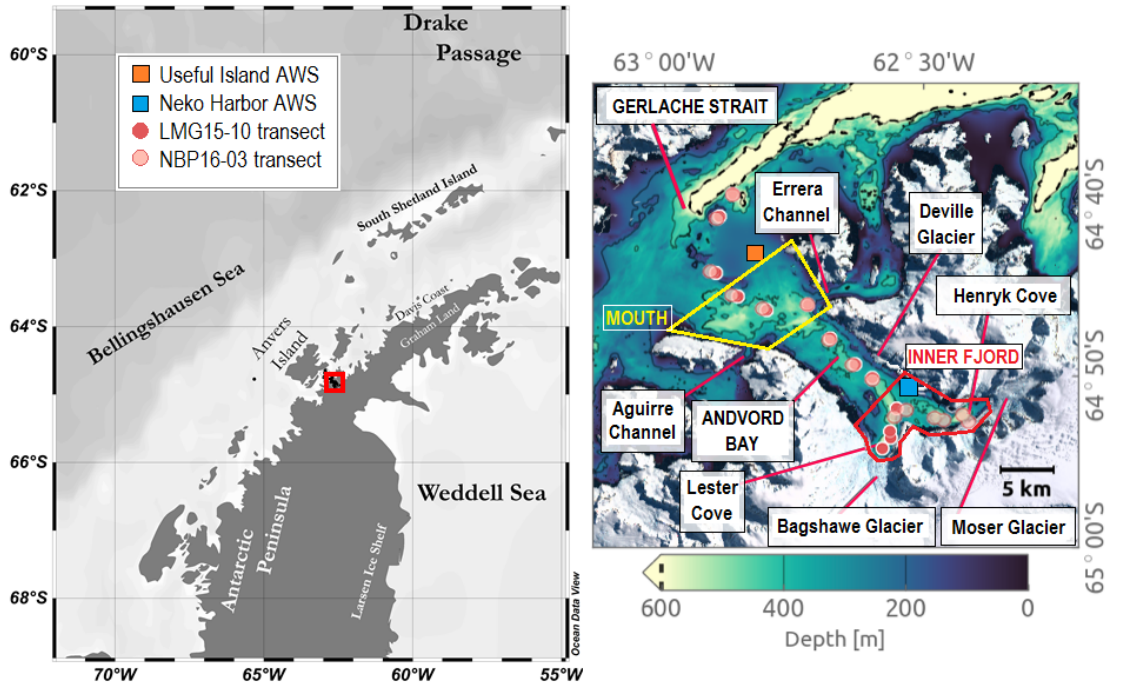

Figure 1: FjordEco study region: Andvord Bay on the Danco Coast of the wAP. Transect stations sampled during cruise LMG15-10, 9-10 December 2015, and NBP16-03, 11-12 April 2016, are indicated by red and pink circles, respectively. The Useful Island and Neko Harbor automated weather station (AWS) installations are indicated with orange and blue squares, respectively. The region referred to as the mouth of Andvord Bay is outlined in yellow and the inner fjord region is outlined in red.

This thesis focuses on sampling performed along fjord from conductivity, temperature, depth (CTD) transects in December 2015 (13 casts) and April 2016 (15 casts). In addition to the synoptic transects with full depth water sampling of macronutrients, the same stations were (re)-occupied during each cruise for a more complete characterization with discrete water sampling for the following analysis: chl-a concentration as an index of phytoplankton abundance, ^{14}C spiked incubations for primary productivity, and oxygen isotopes ($\delta\ ^{18}O$). Seawater samples were collected from Niskin bottles deployed on a rosette sampling system with dual sensors measuring depth, temperature, salinity (Seabird SBE9Plus CTD), fluorescence (WetLabs ECO), and light transmission (QSR-240 from Biospherical Instruments Inc.). CTD data were processed shipboard with standard Sea-bird software version 7.25.0.319.

Samples for macronutrient analysis were collected in acid washed and dried polypropylene tubes that were triple rinsed before filled with seawater. All samples were unfiltered, kept refrigerated in the dark, and were analyzed within 12 hours of collection. Dissolved ortho-phosphate, nitrite, nitrate plus nitrite (N+N), ammonium, and silicic acid were measured using a Lachat QuikChem 8000 flow injection analysis system (Hach Instruments) using modified standard wet-chemistry methods (Gordon *et al.* 1993). NO_3^- concentration was derived by subtracting nitrite from the N+N value.

A calibration was performed to establish the relationship between the fluorometer installed on the CTD rosette and chl-a concentration on each cruise. A volume of water (approximately 140-280 mL, depending on depth) was filtered

through a 25mm GF/F filter, frozen at 80°C, then extracted with 90% acetone for 24 hours at 20°C then analyzed with the standard acidified chl-a method (Parsons *et al.* 1984) on a Turner Designs 10-AU-005 fluorometer calibrated with pure chl-a extracted from Anacystic anidulans (Sigma Co.), with concentration measured spectrophotometrically (Jeffrey and Humphrey, 1975). The linear regression (spring: R^2= 0.84; autumn: R^2=0.80) was used to convert the fluorescence data to mg/m^3 chl-a. Depth-integrated chl-a (mg/m^2) was calculated by integrating chl-a concentrations, converted from CTD fluorescence, to the depth of nutrient depletion, ranging from 50 to 100 m depth.

Primary production from particulate incorporation of 14C was measured after 24-h incubations per Steemann-Nielsen (1952) at 6 depths determined by percent of surface light levels (100%, 50%, 25%, 12%, 6%, 1%). Water was collected in 150 mL UVA/B opaque polycarbonate bottles: 2 light ones, 1 dark and one Time Zero at each light level. Ten µCuries of ^{14}C-labelled bicarbonate were added to each bottle and the t0 samples were preserved immediately. Additionally, at each depth, 100 µL were subsampled into a vial containing 0.1 mL 6N NaOH to estimate the initial 14C-bicarbonate concentration (^{14}C specific activity). All bottles were incubated on deck for 24h, in UVA/B opaque tubes in a UVA/B opaque tank with running seawater from the ship's intake maintaining in situ water temperatures. To simulate the water column light attenuation, screens were placed around tubes holding the 150 mL bottles inside the incubator, with one layer of screen required for approximately each one-half reduction in light level. At the end of the incubation period the bottles were recovered and the sample filtered on Whatman GF/F filters. To release remaining inorganic

14C, 200 µL of 20% HCl were added to each 20-mL scintillation vial containing a filter. Samples were stored at 4°C and after 24 hours, 5 mL of Ultima Gold (Perkin Elmer, USA) were dispensed and each vial was shaken before the 14C activity was measured on the ship in a Perkin Elmer Tri−carb 2900 scintillation counter. Primary production was calculated from the difference between light and dark bottles and integrated to the depth of the 1% light level.

Oxygen isotope samples were collected directly into 30 mL plastic bottles, ensuring no air bubbles were trapped, then sealed securely and stored for less than one year before analysis. The δ18O analysis of water samples was performed at Oregon State University using the water-CO2 equilibration method modified from Epstein and Mayeda (1953). In this method 5 mL of sample (or standard) water was pipetted into a glass bottle. The analysis was calibrated daily with LROSS-6, HOT-4 standards and selected to bracket the expected sample δ18O values. The WAIS-3 low concentration standard was also run as a check. After connection to the equilibration line, vials are left to equilibrate for 15 minutes in an 18°C water bath. Then the headspace of the glass vials is pumped out for approximately 10 minutes, and refilled with CO2 gas. Samples are then left to isotopically equilibrate for 12 hours. Throughout the preparation process, samples were slowly shaken to aid isotopic equilibration. The water is analyzed by dual-inlet mass spectrometry using the DeltaPlus XL with a standard deviation ±0.05 ‰.

Shallow sediments were sampled with a mega-core (12x1 m multi-corer) at each basin station within the study area (depths between 390 m and 567 m). Sediment from the upper 10 cm of one core from each cast was sectioned in 0.5 cm (0-2 cm

depth) and 1 cm (2-10 cm depth) intervals. Approximately 3 cm2 of sediment from the center of each interval, to minimize the effects of light and oxygen exposure, were subsampled into glass vials for pigment analysis. These samples were stored in the dark at -80°C and then freeze-dried; Reuss and Conley (2005) showed this procedure to be suitable for the long-term storage of samples for pigment analysis. Approximately 2 g of each sample were extracted with 90% acetone for fluorometric pigment analysis aboard the ship using the same method as with the water samples. Chl-a concentrations were normalized to the weight of dried sediment, with final units of µg chl-a g-1 sediments.

Between-cruise wind was measured by Antarctic Weather Stations (AWS) with data provided by the University of Wisconsin-Madison's AWS Program. One station was located inside Andvord Bay on the northeastern side of the fjord above Neko Harbor; the other station was located on a small island (Useful Island) in the transition between the mouth of Andvord Bay and the Gerlache Strait (Figure 1). The weather stations measured wind speed and direction every 10 minutes. Shipboard meteorological data was limited to data collected while the vessel was within Andvord Bay (including mouth) with measurements recorded in one-minute intervals. Wind speed was converted to wind stress per Large and Pond (1981) then grouped into 1 hour bins. A threshold of > 0.1 N/m^2 for > 48 hours established from observational effect on stratification was applied to the remaining data to identify additional significant wind events.

Ocean currents determined from hull-mounted acoustic Doppler current profilers (ADCPs) on the LMG were provided by Dr T. Chereskin, Scripps Institution

of Oceanography. Five-minute averaged velocities at 8 m vertical resolution were used to estimate currents along the LMG transect. Data were averaged in depth and time for this analysis.

Nutrient Drawdown Methodology:

To estimate primary production using nutrient drawdown, region-specific nutrient removal assumptions must be made to address inherent unknowns. I combined several variations of the method and underlying assumptions to optimize this method for Andvord Bay. To address the lack of a clear 'winter' reference water to work from, Tremblay *et al.* (2008) and subsequently Bergeron and Tremblay (2014), utilize the 'salinity-nutrient procedure', rather than the typical Jennings' winter water method used in the Weddell Sea. This procedure works to isolate the biologically influenced drawdown by accounting for dilution and by mixing to calculate a corrected 'winter' concentration. The procedure also utilizes variable integration depths to avoid the influence of remineralization.

Priddle *et al.* (1998) presents a similar alternate method in the wAP where winter mixed-layer nutrient concentrations are predicted from profiles exhibiting a minimum in temperature representing the residue of winter water below a summer mixed-layer when annual data (as in Jennings *et al.* 1984) and semi-annual data (as in Priddle *et al.* 1994) are not available. Primary production was estimated from NO_3^- and $SiO4^{2-}$ (autumn only) profiles along the transects. To account for dilution from meltwater, the NO_3^- and SiO_4^{2-} values were normalized to the deep fjord constant salinity value (spring: 34.54 PSU; autumn: 34.51 PSU) using the equation:

$$N_{cor} = (N_{obs} * S_{deep}) / S_{obs} \quad \text{(Eq. 1)}$$

Where: N_{cor}= corrected nutrient concentration
N_{obs}= observed nutrient concentration
S_{deep}= averaged deep salinity concentration along transect
S_{obs}= observed salinity concentration

For depths greater than 150 m in spring and greater than 125 m in autumn, nutrient concentrations were averaged; then deficits were determined by the difference between surface values and the nutrient average at depth. Deficits were then integrated to the depth of intersection between the observed and corrected nutrient values at each site to avoid the influence of remineralization (Bergeron and Tremblay 2014). The integrated value in mmol m^{-2} NO_3^- or SiO_4^{2-} were stochiometrically converted to gC m^{-2} d^{-1}using the Antarctic phytoplankton modified ratio 62:11:1 (C:N:P) by Copin-Montegut and Copin-Montegut (1978) and utilized in Jennings *et al.* (1984) and 4 (C:Si) by Priddle *et al.* (1995) reported for SO phytoplankton.

In summary, the modified nutrient drawdown method utilized in Andvord Bay requires the calculation of nutrient deficit at each sampled depth between the corrected value and the nutrient average at depth. These values are then integrated to the depth of intersection of observed and corrected nutrient value and converted to mgC m^{-2} d^{-1}.

RESULTS

Physical and chemical properties in water column:

In December 2015, potential temperature was observed from -1.26°C to 0.66°C (Figure 2A). The maximum temperature was centered at a depth of 150 m in the Gerlache Strait, setting up both horizontal and vertical temperature gradients. The coldest water was also in the Gerlache Strait at depths greater than 400 m. The warm water from the Gerlache Strait shoals and enters the fjord at a depth of 100 m. Within the fjord (0.6-25 km from the Bagshawe Glacier), the horizontal gradient intensity diminishes along density contours, with the maximum temperature of 0.2°C reaching the surface 18 km from the glacier. The vertical gradient observed in the Gerlache Strait remained within the fjord, with water cooling over a degree from the surface to the bottom. At 100 m depth (27.7 kg/m^3 density contour), the temperature cools from 0°C to -0.5°C towards the glacier over the length of the fjord and fjord mouth (25 km).

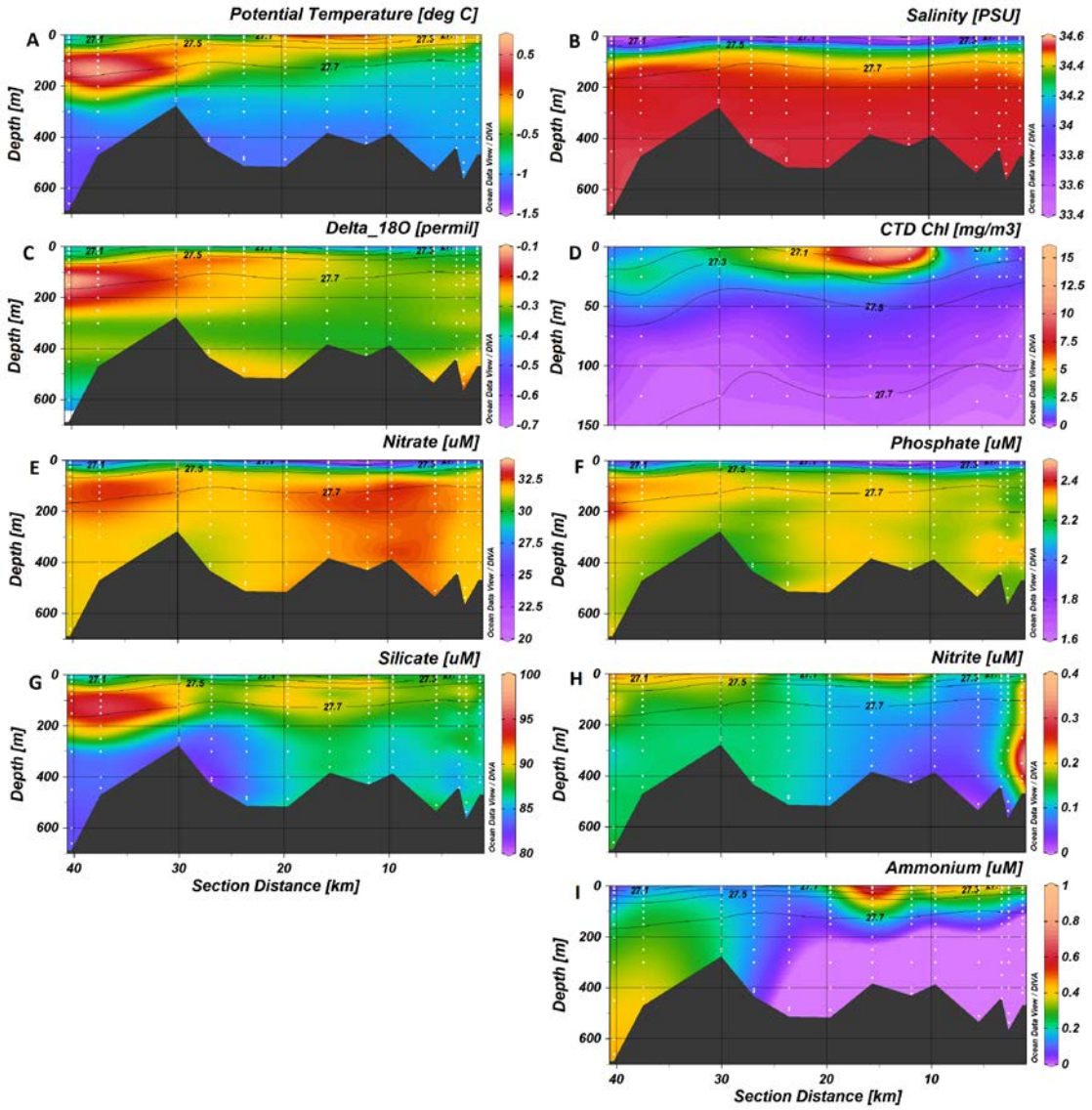

Figure 2 A-I: Late-spring characterization of physical parameters and macronutrient distributions in Andvord Bay: Transect from the inner fjord (0.6 km from Bagshawe glacier) to Gerlache Strait (40 km along transect), 9-10 December with sections illustrating A) Potential Temperature (°C), B) Salinity (PSU), C) $\delta^{18}O$ (‰), D) Chl-a (mg/m^3), E) Nitrate (NO_3^-) (µM), F) Phosphate (PO_4^{3-}) (µM), G) Silicate (SiO_4^{2-}) (µM), H) Nitrite (NO_2^-) (µM), and I) Ammonium (NH_4^+) (µM) with density (kg/m^3) contours overlaid.

Salinity was observed between 33.5-34.6 PSU in early spring with strong vertical gradients in density in both the Gerlache Strait and Andvord Bay (Figure 2B). The density gradient shoals from the Gerlache Strait into the fjord at 30 km, and in the inner fjord at 6 km from the glacier. There was discontinuity in the surface salinity minima, 33.5 PSU and 33.6 PSU, observed at 12 km and 37 km from the glacier, respectively. The maximum salinity of 34.6 PSU was observed at depths below 250 m throughout the fjord.

Delta ^{18}O values ranged from -0.15 ‰ to -0.4 ‰ (Figure 2C). Lower oxygen depletion was observed in the Gerlache Strait at 150 m, corresponding with the temperature maximum in Figure 2A, with values becoming more depleted at the surface (-0.4 ‰) and at depths below 300 m (-0.3 ‰). At depths from 50 m to 275 m there is a minimum in ^{18}O from the Gerlache Strait into the fjord mouth reaching a minimum of -0.3 ‰. Surface waters present more depleted delta ^{18}O at 10 km from the glacier, in association with lower temperatures (Figure 2A). Inside the fjord, the oxygen is depleted near the glacier at 50 m (-0.35 ‰) coinciding with the cold and low salinity surface layer, diluting with distance from the glacier to 5 km.

Chl-a concentrations were highest at the surface (0-50 m) with a maximum of 40 mg/m^2 approximately 10-20 km from the glacier, coinciding with the salinity minimum (Figure 1D). At depths below 150 m concentrations were 0 mg/m^3.

NO_3^- concentrations in late spring ranged from 20.2-32.7 µM (Figure 2E), with lower values at the surface in both the Gerlache Strait (26 µM) and middle fjord (20.2 µM at 12 km from the glacier). Below 75 m there are local maxima, in the Gerlache

Strait at 150 m, at 10 km from the glacier at 200 m, and at 8 km from the glacier at the bottom.

PO_4^{3-} concentrations ranged from 1.61-2.40 µM (Figure 2F), with surface minima of 2 µM in the Gerlache Strait and 1.6 µM in the fjord. Below 75 m there are local maxima, in the Gerlache Strait at 150 m, 14 km from the glacier at the bottom, and 2 km from the glacier at 350 m.

SiO_4^{2-} concentrations ranged from 81.3-94.9 µM (Figure 2G). The maximum SiO_4^{2-} concentration observed was subsurface, centered at 150 m, in the Gerlache Strait, and the minimum was found below 300 m in the outer-fjord (28 km from glacier). In the fjord, the distribution is more uniform with values ranging from 85-90 µM with maxima of 90 µM 18 km from the glacier at 100 m and 11 km from the glacier at 50 m and a minimum of 85 µM 2 km away from the glacier at the bottom.

Low NO_2^- concentrations were observed throughout the study area with values from 0-0.27 µM and local maxima at the surface in the Gerlache Strait (37 km) and 12 km from the glacier, and at a depth of 350 m at 0.6 km from the glacier (Figure 2H).

NH_4^+ concentrations ranged from 0-0.8 µM, with concentration of 0 µM below 200 m in the fjord and a maximum of 0.8 µM at 50 m depth, 14 km from the glacier (Figure 2I).

In April (austral autumn), potential temperature had a range from -0.84°C to 0.23°C, smaller than in December (late spring) (Figure 3A), with warmer deep waters and cooler surface waters. Temperatures warmer than -0.3°C dominated the surface 200 m in the Gerlache Strait (25-43 km from the glacier) with the maximum at 40 m. Temperature decreased with depth with the minimum at the bottom 36 km from the

glacier. The warm (0.23°C) subsurface water enters the fjord at 100 m depth and cools to -0.2°C. In the fjord, a cold-water layer of -0.5°C was observed at 0-20 m depth extending 15 km from the glacier.

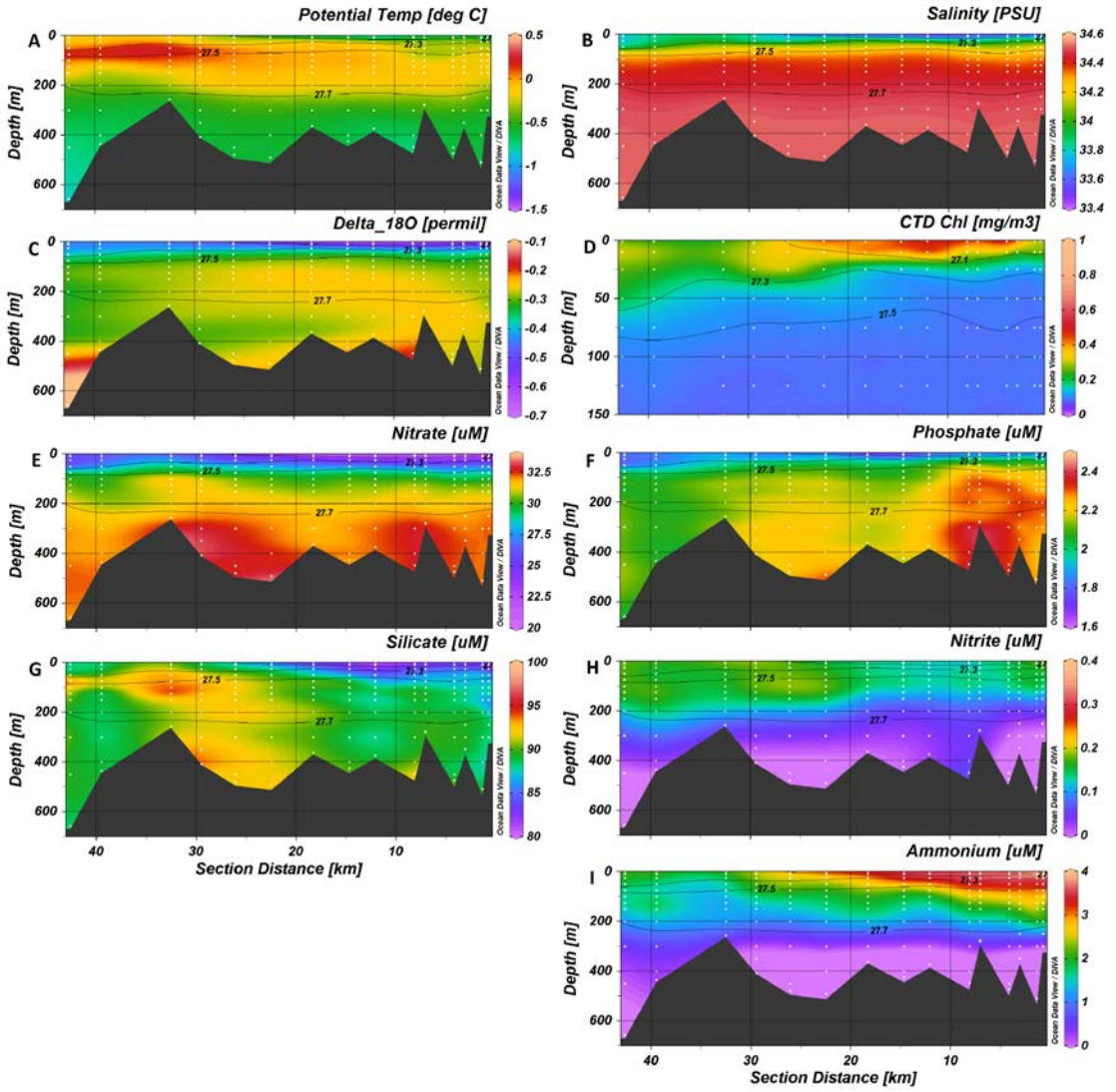

Figure 3 A-I: Autumn characterization of physical parameters and macronutrient distributions in Andvord Bay: Transect from the inner fjord (0.6 km from Moser glacier) to Gerlache Strait (42 km along transect), 11-12 April with sections illustrating: A) Potential Temperature (°C), B) Salinity (PSU), C) $\delta\ ^{18}O$ (‰), D) Chl-a (mg/m^3), E) Nitrate (NO_3^-) (µM), F) Phosphate (PO_4^{3-}) (µM), G) Silicate (SiO_4^{2-}) (µM), H) Nitrite (NO_2^-) (µM), and I) Ammonium (NH_4^+) (µM) with density (kg/m^3) contours overlaid.

Salinity exhibited strong vertical gradients both inside and outside the fjord with values of 33.4 PSU at the surface (maximum at 4 km from glacier) and 34.6 PSU below 400 m depth (Figure 3B). A freshwater lens of < 33.8 PSU occurs at the surface extending from the glacier to 25 km away.

Delta ^{18}O (Figure 3C) values ranged from -0.23 ‰ to -0.66 ‰ with strong vertical gradients following the density contours. The more depleted ^{18}O water was observed at the surface, 11 km from the glacier, and less depleted ^{18}O water at the bottom 0.7 km from the glacier.

High chl-a (Figure 3D) was measured in the 0-75 m surface layer with a max of 40 mg/m^3 at 9 km from the glacier, coinciding with the freshwater and ^{18}O depleted surface lens. At depths below 150 m concentrations were less than 0.1 mg/m^3.

NO_3^- concentrations ranged from 21.9-33.3 µM (Figure 3E). Decreased concentrations (21.9-26 µM) were observed in the surface waters (0-60 m) in both the Gerlache Strait and inside the fjord with lower values closer to the glacier, increasing towards the Gerlache Strait. Deep NO_3^- concentrations, below 200 m, were 32-33.3 µM with maxima at the bottom at 8 km and 30 km from the glacier.

PO_4^{3-} concentrations ranged from 1.70-2.42 µM (Figure 3F). In both the Gerlache Strait and inside the fjord, surface minima of 2 µM in the Gerlache Strait (42 km from the glacier) and of 1.6 µM in the middle fjord (8-12 km from the glacier). Below 75 m there are local maxima, in the Gerlache Strait at 150 m, 14 km from the glacier at the bottom, and 2 km from the glacier at 350 m.

SiO_4^{2-} concentrations ranged from 81.3-94.9 µM (Figure 3G). The maximum was observed at subsurface at 150 m in the Gerlache Strait and minimum value below

300 m in the outer fjord (23 km from glacier). Inside the fjord, the distribution is more uniform with values ranging from 85 µM to 90 µM, with maxima of 90 µM 18 km from the glacier at 100 m, and 11 km from the glacier at 50 m and a minimum of 85 µM at the bottom 2 km from the glacier.

Low NO_2^- concentrations were observed throughout the study area with values from 0-0.21 µM with local maxima in the surface to 100 m layer in the Gerlache Strait (42 km from the glacier) and 26 km from the glacier and less than 2 km from the glacier (Figure 3H).

NH_4^+ concentrations ranged from 0-3.85 µM with vertical and horizontal gradients (Figure 3I). The maximum of 3.85 µM was observed at the surface near the glacier (0.6-5 km) decreasing to 2 µM at the surface at a distance 30 km from the glacier. No ammonium was observed below 300 m in the fjord and 400 m in the Gerlache Strait.

Wind and currents:

Andvord Bay is more quiescent than the Gerlache Strait. Hourly averaged currents measured from shipboard ADCP were < 10 cm/s inside the fjord and up to 30 cm/s in the Gerlache Strait at a depth of 62.5 m (Figure 4A). Wind stress observed from the AWS installations is consistently greater in magnitude and duration in the Gerlache Strait than in Andvord Bay by a factor of 4 (Figure 4B). The Useful Island (Gerlache Strait, 30 km from glacier) AWS installed from 15 December 2015 to 6 March 2017 measured wind stress of 0-1.24 N/m^2 and the Neko Harbor installation from 19 December 2015 to 8 February 2017 determined values half as high, from 0 N/m^2 to 0.68 N/m^2 (Figure 4B).

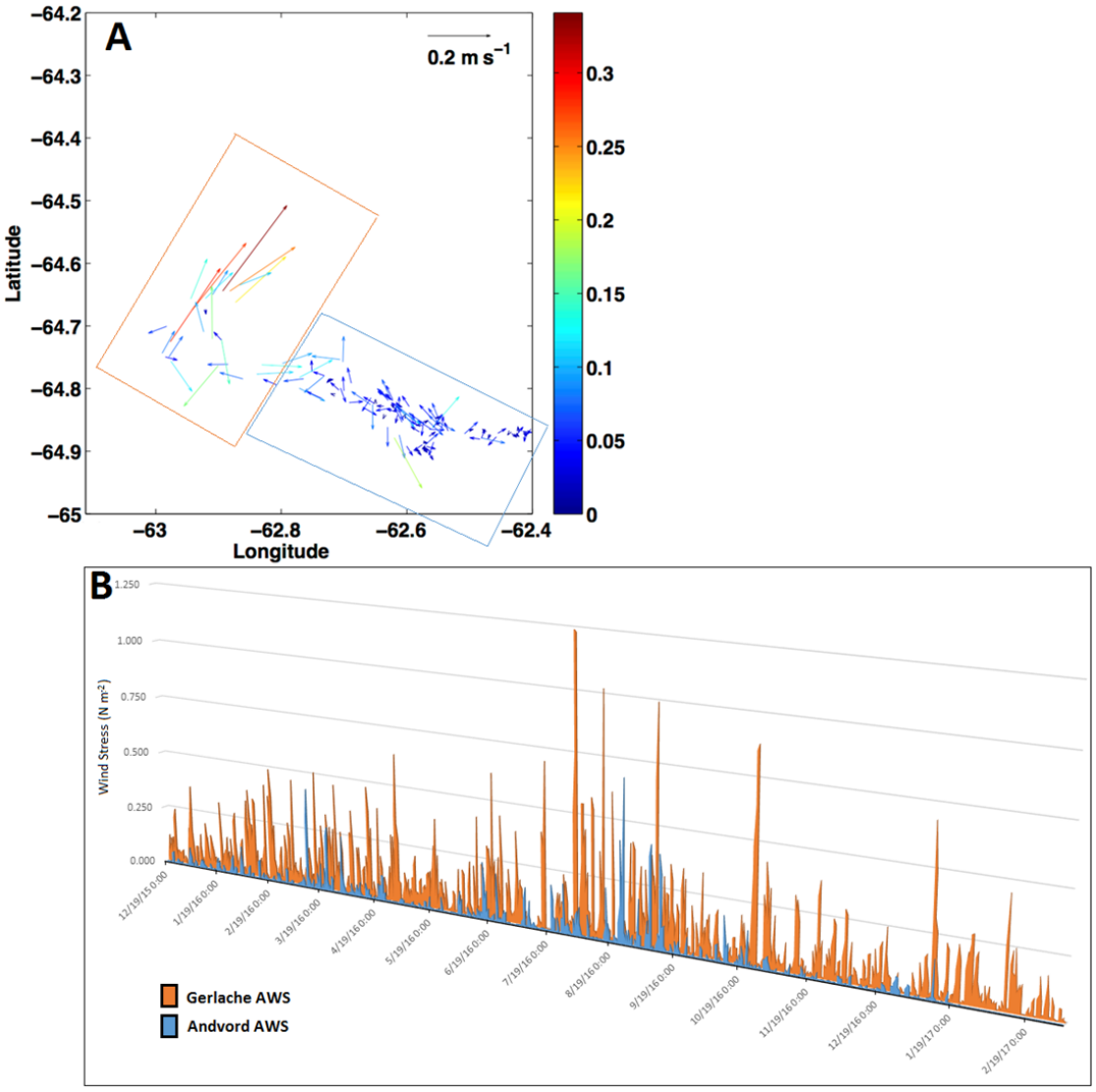

Figure 4 A-B: Comparison of currents and wind stress in the Gerlache Strait and Andvord Bay: A) Hourly averaged currents at 62.5 m depth plotted every 4 hours in the Gerlache Strait and Andvord Bay, 27 November to 19 December 2015 and B) Wind stress (N/m^2) from AWS stations on Useful Island in the Gerlache Strait (Orange) and in Neko Harbor in Andvord Bay (Blue), December 2015 to February 2017.

Shipboard wind data from within Andvord Bay, binned hourly, yielded wind stress from 0.0-2.03 N/m^2 in Spring 2015 (Figure 5A) and 0.0-0.785 N/m^2 in autumn 2016 (Figure 5B). Early on 10 December 2015, winds built causing wind stress to surpass 0.1 N/m^2 and generally remain elevated for more than 80 hours with a maximum wind speed of 28 m/s reached the night of 12 December 2015. The wind started out of the south then came around to the southeast blowing along and out of Andvord Bay. Between cruises, the AWS data shows a quieter fjord with low winds until autumn (late March 2016) when three bursts of wind generated a wind stress of up to 0.47 N/m^2. The events on 29 March 2016 and 6 April 2016 both sustain > 0.1 N/m^2 stress for 24 hours (Figure 5C). The greatest wind stress recorded with the AWS occurred in winter (July and September 2016) with hourly binned wind stress reaching 1.7 N/m^2. Increased wind event durations were observed between July and October 2016 (Figure 5C).

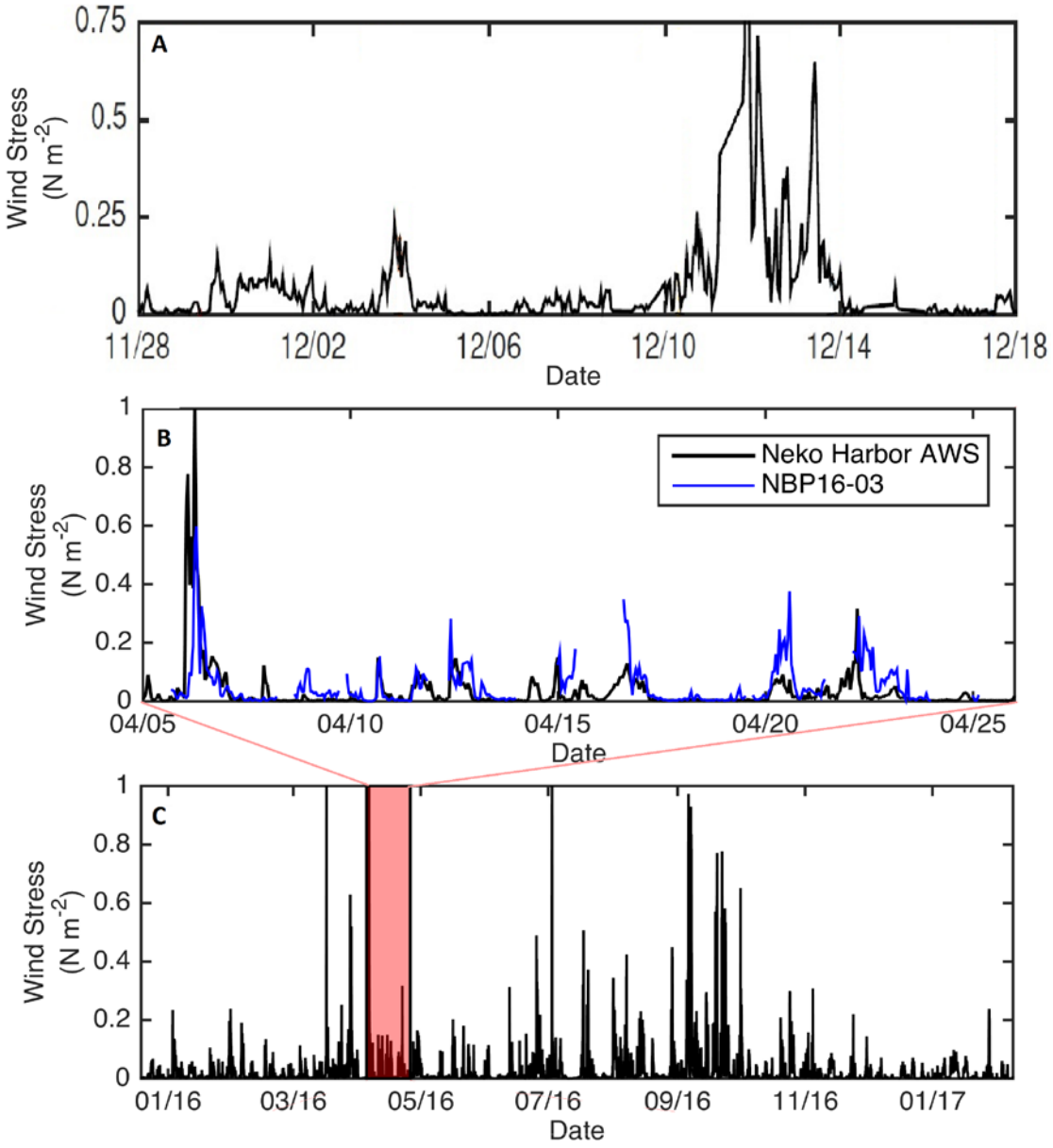

Figure 5 A-C: Wind forcing in Andvord Bay: Hourly binned wind stress (N/m^2) from shipboard measurements in the Andvord Bay A) LMG1510 B) NBP1603 (in blue), directly compared to measurements observed for the same time period by the Neko Harbor AWS installation (in black) and C) AWS from Neko Harbor from its installation in 19 December 2015, through removal in 08 February 2017, with the time period data simultaneously collected on NBP16-03 highlighted in pink.

Response of nutrients to wind events:

Repeated sampling of a mid-fjord station, approximately 10 km from Bagshawe Glacier, indicated temporal variation in stratification and vertical NO_3^- gradient related to wind stress (Figure 6A). This station showed a stable 50 m surface layer (Figure 6B) between 29 Nov and 04 December, with a consistent subsurface chl-a maximum of nearly 6 mg/m^3 at 10 m (Figure 6C) and a decrease of 2.4 µM NO_3^- (Figure 6D) in this time period. From 04 to 10 December the surface layer (0-50 m) became more stratified, with a decrease in surface chl-a from 6 mg/m 3.1 mg/m^3 and NO_3^- reaching a minimum of 23.7 µM. On 13 December, towards the conclusion of the storm of 10-13 December (Figure 6A), a loss of stratification and vertical gradients were observed in the surface to 50 m layer, with surface density of 27.6 kg/m^3, chl-a of 0.01 mg/m^3, and NO_3^- replenished to 32.5 µM. On 17 December, a return of stratification was observed as well as an increase of sub-surface chl-a to 4.1 mg/m^3 corresponding with a 4.1 µM NO_3^- drawdown. There is negligible change observed through this sequence in the SiO_4^{2-} profiles (Figure 6E) and the observed variation at each depth is within the analytical error of the instrument.

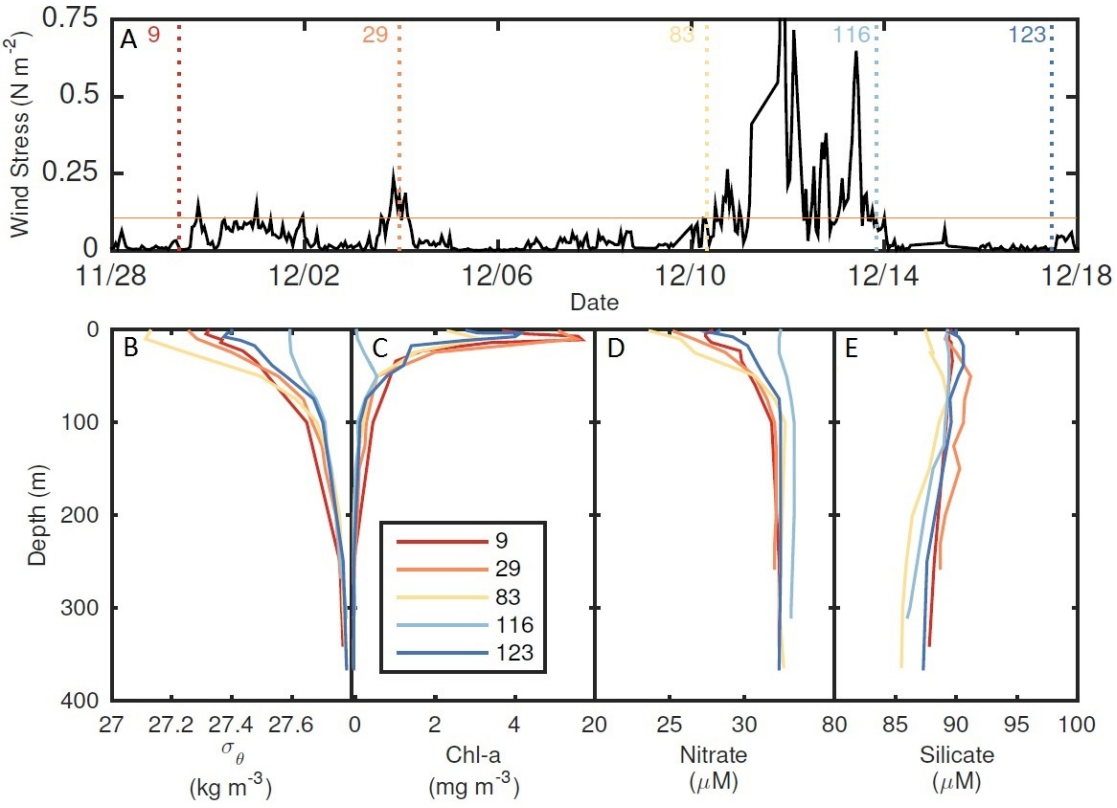

Figure 6 A-E: Effects of wind event: A) Wind stress from LMG15-10 with 0.1 N/m^2 threshold in orange and corresponding variation observed in B) Potential density, C) Chl-a, D) NO_3^-, and E) SiO_4^{2-} profiles at a sampling station in Andvord Bay approximately 10 km from Bagshawe Glacier, between 28 November and 17 December 2015. Colors and corresponding numbers represent distinct CTD casts.

During two 24-hour sampling periods in neap and spring tides, local nutrient variability was assessed. With moderate wind, out of the northwest, the dominant flow from hourly averaged ADCP data on 04 December 2015 in the mid-fjord was to the northwest in the 37-100 m layer with max speed of 4 cm/s at 62 m, with diminishing speed to < 2 cm/s below 150 m with Southwest direction (Figure 7A). During the 24-hour period with this current pattern, there was a pulse providing a 2 µM replenishment from 25 µM to 27 µM of surface NO_3^- associated with a 0.16 PSU freshening and dilution of the surface chl-a (Figure 7B). This pulse brought water with reduced SiO_4^{2-}. Following the pulse there was a return to high SiO_4^{2-} (94 µM) water in the surface to 150 m layer (Figure 7D). After the strong wind event of 10-13 December over an 18-hour 'high tide' current cycle, the dominant current recorded with ADCP approached 5 cm/s flowing into the fjord at depths of 37-150 m and diminishing in strength to 0 cm/s at 200 m (Figure 7E). NO_3^-, already replenished to 31 µM saw further increases with values increasing 0.5 µM at 100 m and 1 µM at 300 m. After 12 hours, the additional replenishment had reached the surface with an increase of 1.5 uM at the surface where concentrations were 32.5 µM. At the same time, there was a deepening of the surface chl-a concentration (0-50m) to subsurface (25-75m) (Figure 7F). The SiO_4^{2-} profiles indicate subsurface concentration increases at 75-100 m water at 3 hours and at 14.5 hours (Figure 7H).

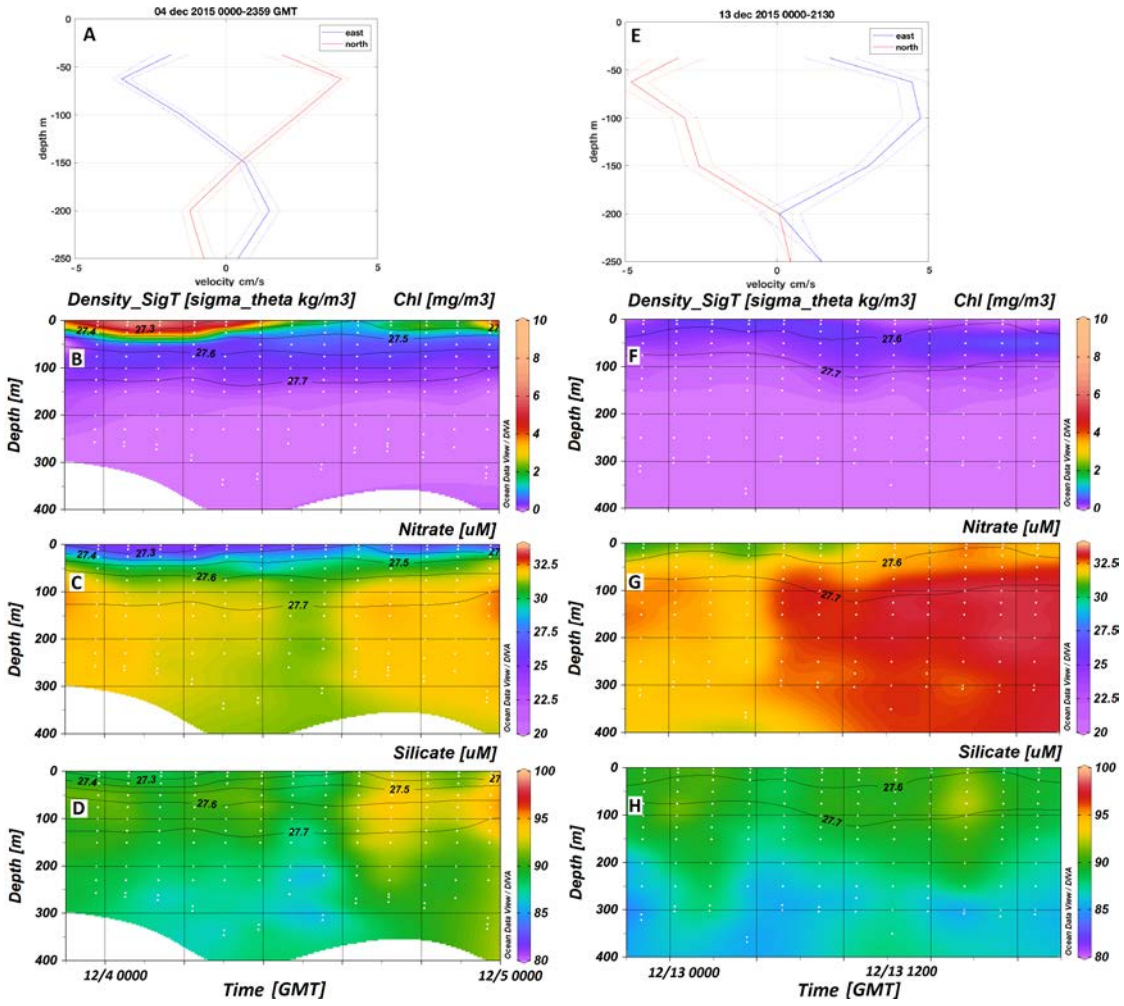

Figure 7 A-H: Mid-fjord tidal stations: Temporal comparison of repeated occupation approximately 12 km from glacier on two dates, 04 and 13 December 2015. For 04 December A) averaged ADCP profiles for depths 37.5 to 250 m with standard error as dotted lines, B) Chl-a (mg/m^3), C) NO_3^- (µM), and D) SiO_4^{2-} (µM) profiles over the approximately 24 hours on station with density contours overlaid. For 13 December E) averaged acoustic Doppler current profile (ADCP) profiles for depths 37.5 to 250 m with standard error as dotted lines, F) Chl-a (mg/m^3), G) NO_3^- (µM), and H) SiO_4^{2-} (µM) profiles over the approximately 21 hours on station with density contours overlaid.

Nutrient ratios:

The NO_3^- to PO_4^{3-} ratio in spring (Figure 8A) is linear paralleling the expected Redfield ratio (Redfield *et al.* 1963) of 16:1. The lowest SiO_4^{2-} values in color on the plot are towards the higher NO_3^- and PO_4^{3-} at the surface identifying the low SiO_4^{2-} water Weddell Sea Deep Water (WSDW). In autumn, the NO_3^- to PO_4^{3-} ratio is still linear with a steeper slope and the lowest SiO_4^{2-} values associated with the drawn down NO_3^- and PO_4^{3-} values (Figure 8C).

In spring, the SiO_4^{2-} to NO_3^- ratios show two features (Figure 8B). Samples with low density (i.e., surface) indicate decreasing NO_3^- and stable SiO_4^{2-}. There is a horizontal set of decreasing NO_3^-, stable SiO_4^{2-} and low density associated with surface water and non-diatom growth. There is also a gradient in SiO_4^{2-} with stable NO_3^- and density greater than 27.5 kg/m^3, corresponding to mid- and deep waters. The SiO_4^{2-} to NO_3^- ratio in autumn (Figure 8D) is linear with an approximately 1:1 ratio, the density of these samples indicates the maximum drawdown was in the surface water.

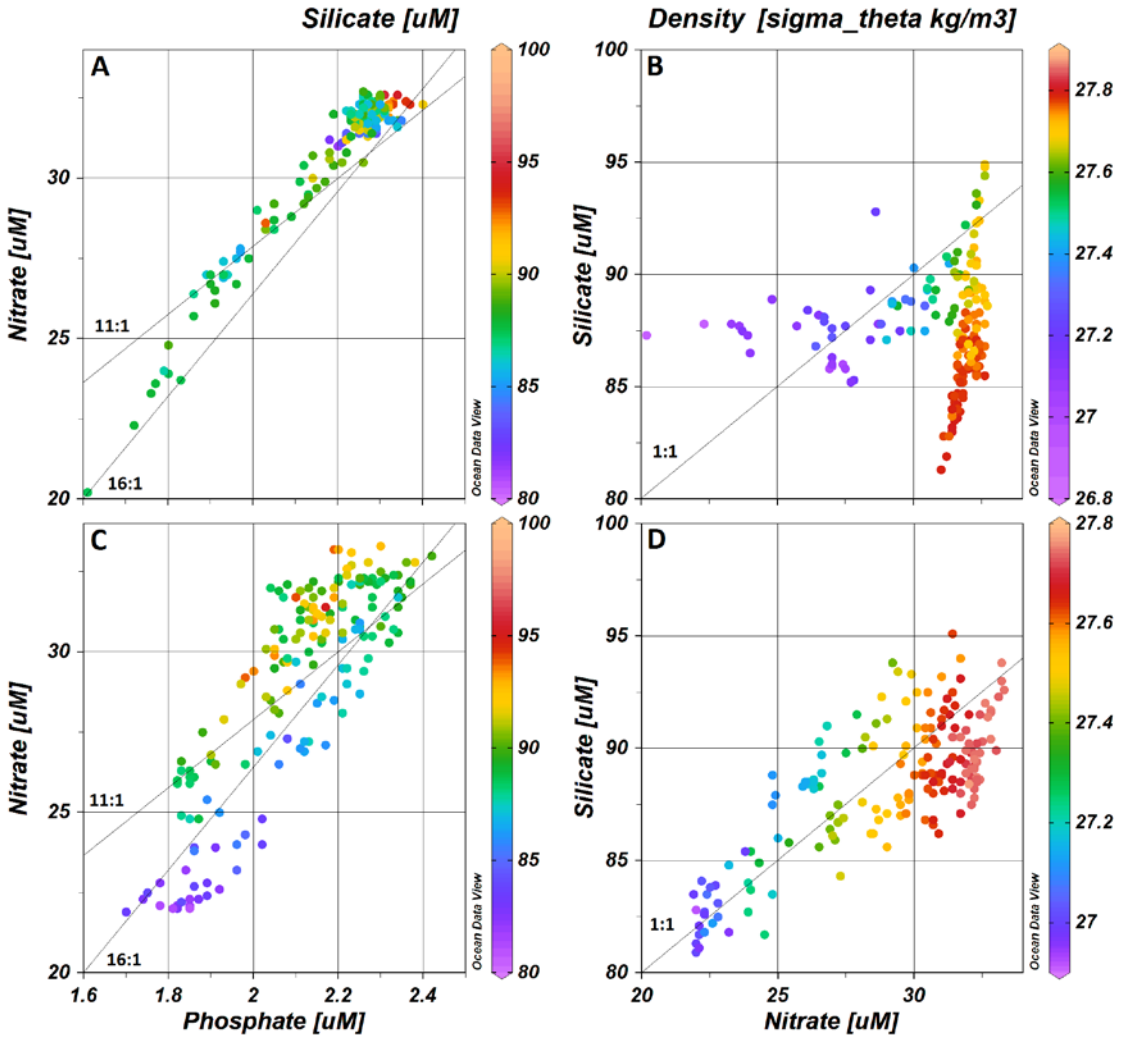

Figure 8 A-D: Comparison of nutrient ratios: NO_3^- to PO_4^{3-} ratios, with SiO_4^{2-} concentration in color, along a transect from the inner fjord to the Gerlache Strait A) Spring 2015 and C) Autumn 2016 with 11:1 and 16:1 ratio reference lines. SiO_4^{2-} to NO_3^- ratios from the same transects with density in color B) Spring 2015 and D) Autumn 2016 and 1:1 ratio reference line.

Estimating primary production:

Using 15 October 2015 as the start of the 2015-16 growth season allowed for a 55-day period of nutrient depletion before the field sampling in spring. With the integrated nutrient deficit approach, primary production conservatively ranged from 75-292 mgC m^{-2} d^{-1} along the transect until 9-10 December (Table 1). Production was low in the inner fjord, increased to a maximum in the mid-fjord (15-18 km) and then reached a minimum in the fjord mouth (33 km) with a slight increase in the middle of the Gerlache Strait (Figure 9A). In contrast, primary production through 24-hour incubation from 29 November to 10 December ranged from the minimum 300 mgC m^{-2} d^{-1} in the inner fjord 3 km from the glacier, increasing to the maximum of 3563 mg C m^{-2} d^{-1} in the fjord approximately 16 km from the Bagshawe Glacier. Integrated chl-a concentrations ranged from 30 mg m^{-2} to 267 mg m^{-2} and followed the same pattern as the primary production estimates, low in the inner-fjord, reaching a maximum at the fjord mouth, then falling to a mid-range value in the Gerlache Strait.

Table 1: Summary of spring production: Primary production estimates and chl-a representing biomass from spring 2015 along transect from the Bagshawe Glacier in Andvord Bay to the Gerlache Strait. Production by drawdown assumes a 55-day growth period, from 15 October 2015 to discrete sampling on 10 December 2015.

Distance from glacier (km)	mgC m^{-2} d^{-1} by drawdown (NO_3^-)	Integrated chl-a (mg m^{-2})	Date of ^{14}C Incubation	mgC m^{-2} d^{-1} by ^{14}C incubation
40.3	129.86	78.1	12/11/2015	3250
37.5	184.73	99.9		
30.0	75.47	82.7		
26.9	114.83	96.6		
23.6	186.15	155.9	12/12/2015	2572
19.6	169.39	164.2	12/9/2015	1786
15.6	287.45	267.8	12/1/2015	3563
11.9	292.24	212.0	12/7/2015	523
9.6	259.53	83.4	11/29/15	1319
5.5	252.34	49.4		633
3.3	130.42	49.7	11/30/2015	966
2.7	177.36	34.4	12/2/2015	300
1.3	103.93	30.0	12/5/2015	524

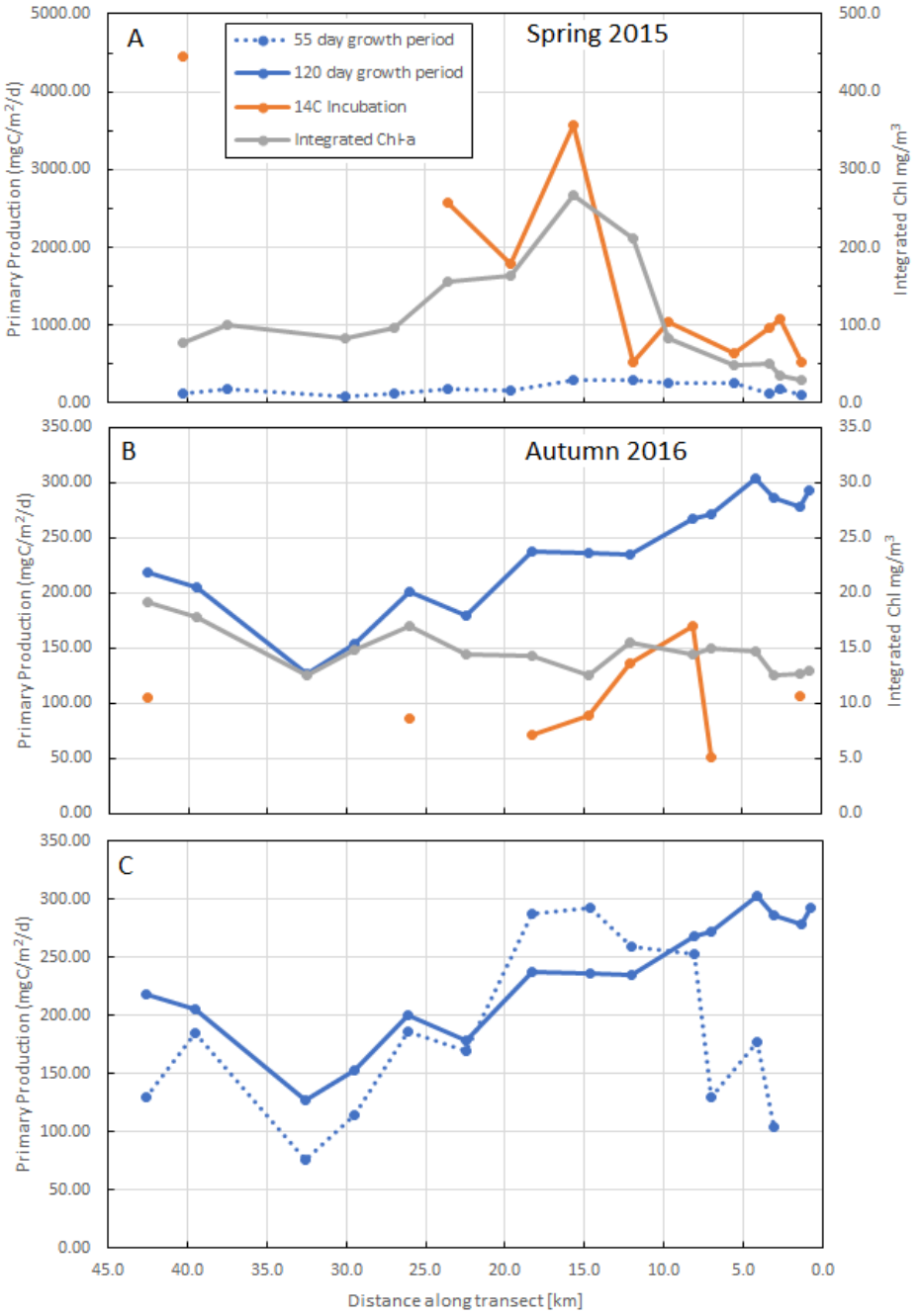

Figure 9 A-C: Integrated primary production and biomass estimates: Primary production estimates (left axis) and integrated chl-a (right axis) from the Gerlache Strait (> 30 km) to near the inner fjord glacier (0 km) for A) spring 2015 and B) autumn 2016. The 55-day growth period is from 15 October 2015 to 10 December 2015 and the 120-day growth period is 13 December 2015 to 12 April 2016. On both plots, chlorophyll-a is integrated to the same depth as the nutrient drawdown and ^{14}C incubation values are from the discrete, 24 hour ^{14}C uptake incubations. A direct comparison of the primary production estimates from the two growth periods in C).

With the AWS data indicating no additional major wind events between 13 December 2015 and the field sampling in autumn (11-12 April 2016) the conservative estimate for primary production with a 120-day growth season estimated rates between 127 and 303 mgC m^{-2} d^{-1} (Table 2, Figure 9B) with the maximum in the inner-fjord and decreasing to the minimum in the mouth followed by an increase to greater than 200 mgC/m^2/d in the Gerlache Strait. Incubation experiments from 4-22 April determined a range of production from 50 to 170 mgC m^{-2} d^{-1}, with the maximum and the minimum in Andvord Bay approximately 8 km and 7 km from the Moser Glacier, respectively. Integrated chl-a concentrations ranged from 12 to 19 mg m^{-2} with a maximum in the Gerlache Strait and minima at the mouth of the fjord and in the inner-fjord.

The drawdown method presenting a seasonal integration shows an increase in rates from spring to autumn and a change in pattern, with the greatest values shifting from the middle of the fjord to the inner-fjord, with the maximum at 4 km from glacier (Figure 9C).

Table 2: Summary of autumn production: Primary production estimates and chl-a representing biomass from autumn 2016 along transect from the Moser Glacier in Andvord Bay to the Gerlache Strait. Production by drawdown assumes a 120-day growth period from 13 December 2015 to discrete sampling on 11 April 2016.

Distance from glacier (km)	mgC m^{-2} d^{-1} by drawdown (NO_3^-)	mgC m^{-2} d^{-1} by drawdown (SiO_4^{2-})	Integrated chl-a (mg m^{-2})	Date of ^{14}C incubation	mgC m^{-2} d^{-1} by ^{14}C incubation
42.6	218.22		19.1	4/15/2016	105.4
39.5	205.50		17.9		
32.5	127.17		12.6	4/21/2016	
29.5	153.27		14.9		
26.1	200.47		17.0	4/18/2016	86.2
22.5	178.85		14.4		
18.3	237.97	62.89	14.3	4/6/2016	71.4
14.7	235.62	85.39	12.6	4/14/2016	89.6
12.1	234.85	159.13	15.5	4/16/2016	137.3
8.1	267.91	68.56	14.4	4/10/2016	170.3
7.0	271.41	124.55	15.0	4/13/2016	51.4
4.1	303.33	107.61	14.7		
3.1	286.32	127.11	12.6	4/20/2016	
1.3	278.70	108.26	12.6	4/18/2016	106.9
0.7	292.90	153.16	12.9		

DISCUSSION

The data presented herein are a representative subset of data collected on the FjordEco cruises and the macronutrients concentrations observed (Table 3) agree with previous estimates in the wAP region (Dore and Karl, 1992, Smith *et al.* 1999, Ducklow *et al.* 2007). Although surface nutrient deficits were observed during both seasons, there was no indication of N or Si limitation, with surface concentrations remaining greater than 20 µM (NO_3^-) and 80 µM (SiO_4^{2-}), respectively (Serebrennikova and Fanning 2004). PO_4^{3-} concentrations followed NO_3^- except for indications of enrichment from sediments in the inner-fjord in autumn. Nitrite concentrations, save one elevated subsurface inner-fjord value, remained less than 0.27 µM throughout the year. Ammonium was less than 0.9 µM during the spring, then exhibited a factor of 4 increase in surface concentrations by the autumn, an indication of late season zooplankton grazers in Andvord Bay (Lehette *et al.* 2012). NO_3^- to PO_4^{3-} ratios indicated uptake following the Redfield 16:1 ratio, not the expected modified ratio of 11:1 (Copin-Montegut and Copin-Montegut 1978). It is not clear if the change in N:P ratio implies a shift in the C:N uptake ratio; for this reason, the 62:11 C:N ratio was still utilized for the estimation of primary production (Priddle *et al.* 1998). SiO_4^{2-} to NO_3^- ratios were dominated by physical processes in the spring, shifting to a more biologically influenced ratio by the autumn sampling.

Table 3: Macronutrient comparison: Dissolved inorganic macronutrient concentration ranges and ratios.

	Spring 2015 (28Nov to 24Dec)	Autumn 2016 (28Mar to 28Apr)
Phosphate (PO_4^{3-})	1.61-2.4	1.7-2.42
Nitrite (NO_2^-)	0.094-0.27	0.04-0.21
Ammonium (NH_4^+)	0.114-0.886	0.07-3.85
Silicate (SiO_4^{2-})	81.3-94.9	80.9-95.1
Nitrate (NO_3^-)	20.2-32.7	21.9-33.3
NO_3^- : PO_4^{3-}	12.55-14.61	11.77-15.69
SiO_4^{2-} : NO_3^-	2.62-4.32	2.72-3.81

The Gerlache Strait may exhibit seasonal and annual variation in the presence of UCDW flooding onto the continental shelf from the west (Martinson and McKee 2012) and Bransfield Strait Water (BSW), influenced by water masses of the Weddell Sea, which flows from the north (Smith *et al.* 1999, Cook *et al.* 2016). These water masses are the source of nutrients to Andvord Bay. The estimated primary production from NO_3^- drawdown represented total phytoplankton growth; the estimates drawn from SiO_4^{2-} depletion represented the portion of this production attributed to diatoms. Ephemeral, intense blooms of diatoms with high productivity are balanced by low winter activity, generating moderate annual productivity estimates that can be described by the drawdown method (Jennings *et al.* 1984). The low biomass observed in the inner-fjord in December and April are unlikely to be representative of the biomass in that region during a short, intense blooms. This supports the need for a seasonal estimate to more accurately represent primary production in Andvord Bay.

Nutrient Distribution:

Nutrient concentrations are both physically and biologically influenced. Winter deep mixing in high latitude regions brings macronutrients up to the surface water, with the winter mixed layer persisting “winter” concentrations under seasonal ice. As conditions for phytoplankton growth become optimal due to retreat of sea ice, meltwater accumulation and increasing light, phytoplankton in the stable surface layer can take up the available nutrients and bloom. During this growth period a trace of the winter water remains below the summer mixed layer, identified by a higher salinity and lower temperature signature than the surface waters.

In Andvord Bay, however, a subsurface winter water layer was not apparent; rather, two potential source water masses converging in the Gerlache Strait were identified. The characteristics of the water sampled around Andvord Bay indicate modification from the standard wAP shelf water masses of Martinson *et al.* (2008) (Figure 10). Andvord Bay opens into the Gerlache Strait, which can be considered a transitional region of the wAP shelf waters. In the Gerlache Strait, distinct water masses are present that vary seasonally and influence the hydrography of the fjord. Fjords to the south of Andvord Bay are exposed to lower air temperature and warmer ocean deep water than the fjords further north (Cook *et al.* 2005, 2016). The deep water is characterized by the influence of WSDW on Bransfield Strait Water (BSW) in the north, a cold, low SiO_4^{2-} water mass from the Weddell Sea that flows down the peninsula, and UCDW in the south, a warm, nutrient rich water mass that floods the continental shelf and enters the Gerlache Strait from the south. In December 2015, both these water masses were observed in the Gerlache Strait (Figure 2). The subsurface (< 200 m) presence of nutrient-rich modified UCDW (mUCDW), which can be traced by its temperature, appears to be the primary source of early season nutrients to Andvord Bay. It is unclear if the BSW can penetrate Andvord Bay or if it is blocked by an outer sill at the fjord mouth; the distinct silica signature (< 85 µM) indicates it may not advance past the mouth of Andvord Bay (Figure 2G).

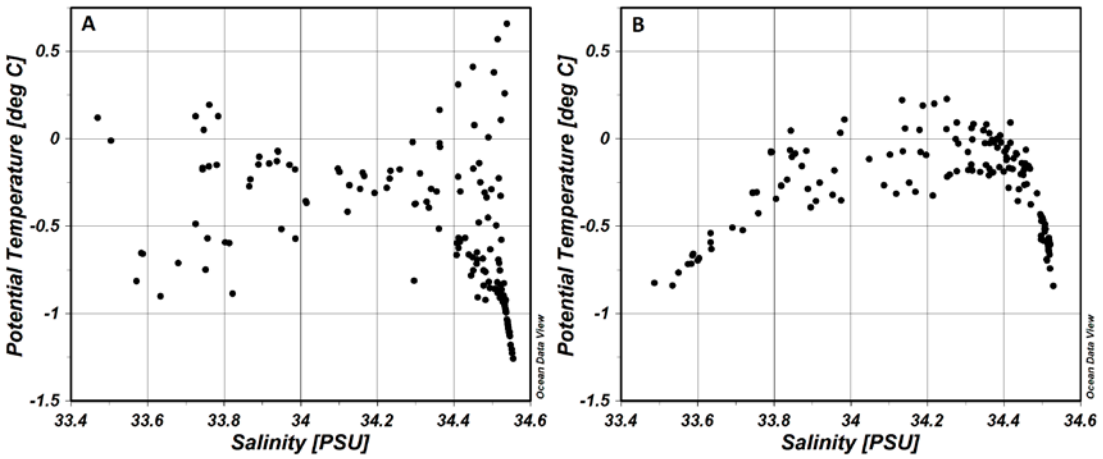

Figure 10 A-B: Comparison of T-S diagrams: A) Spring 2015 and B) Autumn 2016

Both these water masses have similar NO_3^- and PO_4^{3-} signatures and their combination influences the baseline macronutrient concentrations in Andvord Bay, including the deep concentrations that were averaged and used as the baseline concentrations in lieu of winter water. The SiO_4^{2-} signature of the mUCDW is also distinct (> 90 µM) causing a subsurface (density 27.5-27.7 kg/m^3) maximum throughout the transect in spring as the source water disperses in the fjord (Figure 8). An additional source of macronutrients to Andvord Bay is remineralized organic material, both excreted by phyto- and zooplankton and dissolution from sediments. Surface SiO_4^{2-} depletion decoupled from NO_3^- can be an indication of a deep silica source enriching differentially surface water, potentially opal dissolution from the sediments (Gordon *et al.* 2000). The December decoupling of NO_3^- to PO_4^{3-} and SiO_4^{2-} at depth (approximately 15 km from the glacier) supports the possibility of dissolution of nutrients from the sediment at the sills. The NO_3^- to SiO_4^{2-} ratio of 1:1 in April 2016 indicates Fe replete growth (Brzezinski and Nelson, 1995). Advection, vertical mixing, and diffusion can bring nutrients from these local sources into the euphotic zone. The input of NO_3^- to the system from an external source through advection or vertical mixing would allow for increased new production, while production from remineralized or excreted nitrogen (NO_2^- or NH_4^+) would be considered recycled production.

Little is known about the seasonal progression of phytoplankton assemblages in Andvord Bay. To date, research along the wAP demonstrates that diatoms tend to dominate summer blooms though small phytoplankton are also important for annual primary production along the wAP (Garibotti *et al.* 2005; Clarke *et al.* 2008). Indeed,

shifts in dominant species with bloom progression are expected throughout the season as the species best-suited for the current conditions tend to dominate until they become limited in their ability to grow, or are consumed (Mendes *et al.* 2013). In oligotrophic and seasonal upwelling regions, pulses of macronutrients to the surface lead to a shift in dominant species from small to large phytoplankton (Bibby *et al.* 2008; Brown *et al.* 2008; Mouriño-Carballido, 2009; Vaillancourt *et al.* 2003). It is unclear why the abundance of macronutrients in spring in Andvord Bay does not initiate a similar bloom progression starting with diatoms when light and a stable surface layer are available. Since the Andvord Bay system does not reach macronutrient limitation, diatom dominance may be dependent on something other than macronutrients. The considerable biomass observed in December 2015 (maximum > 250 mg chl-a m^{-2}, Table 2) suggests that phytoplankton growth had already been occurring and the measured nutrients concentrations in December were biologically influenced. The order of magnitude decrease in observed biomass in April is not unexpected late in the season, but the presence of biomass confirms the persistence of the growth season. Nutrients incorporated into biomass can be exported from the euphotic zone and be re-mineralized while sinking or reach the benthos where they are consumed or buried.

Primary Production Estimated from Nutrient Drawdown:

Deficits of NO^{3-} give comparable primary production estimates in both time periods considered, 15 October to 10 December 2015, and 13 December 2015 to 12 April 2016, with values ranging from 75 to 303 mgC m^{-2} d^{-1} (Figure 9C). Greater primary production rates were estimated within the inner-fjord of Andvord Bay in comparison to the mouth, with intermediate values in the Gerlache Strait. In the

spring, maximum production and biomass was measured in the middle of the fjord. This could reflect light limitation due to brash ice cover in the inner-fjord, with these inner waters not clearing as early as further away from the glaciers. From December to April, more production occurred in the inner fjord. Although the transects sampled different inner basins, additional sampling during the cruises confirmed the seasonal difference between the two areas: even though the southern Lester Cove with Bagshawe Glacier was sampled in spring and the northern Henryk Cove next to Moser Glacier in autumn, both experienced a shift in maximum production from the middle- to inner-fjord during the growth season. Sampling in Henryk Cove four days before the spring 2015 transect indicated surface NO_3^- of 27.5 µM and chl-a 1.03 mg m^{-3}; while these nutrient concentrations indicate slightly more growth than Lester Cove, they do not change the overall trend of maximum growth 15 km from the glacier in the middle-fjord with surface NO_3^- of 20.2 µM and chl-a 15.25 mg m^{-3}. In autumn 2016, surface samples in Lester Cover six days after the Henryk Cove transect sampling showed NO_3^- of 25.6 µM and chl-a 0.3 mg m^{-3}, indicating slightly less surface nitrate depletion throughout the season than in Henryk Cove but did not change the trend of increasing primary production estimates approaching the inner-fjord.

The estimates from the two periods suggest at least a six-month growth season in Andvord Bay, still active in mid-April, with the potential to fix at least 81 g C m^{-2} throughout the season, or a total of 30 Tons of C. The method of integration used includes “all” biologically modified waters, to account for local mixing, turbulence, and diffusion that could distribute the depletion from the euphotic zone into a deeper layer. The additional depth included in deficit integration does introduce the

possibility of overestimating phytoplankton growth due to drawdown from bacteria utilizing nutrients below the euphotic zone. Based on Bergeron and Tremblay (2014), a salinity correction of the nutrient concentrations was used to identify an integration depth minimizing the influence of remineralization. The similarity in values calculated between both the early and late season, as well as comparability to other values from the wAP, support the use of this modified method (Table 4).

Table 4: Comparison regional methods and results: A summary of NO_3^- deficit and C estimates in Antarctic regions with varying methods of primary production estimation.

	Region	Method	NO_3^- Deficit	C estimate
El-Sayed & Taguchi	Weddell Sea	^{14}C incorporation		104-410 mg C m^{-2} day^{-1}
Jennings *et al.* 1984	Weddell Sea	Nutrient Deficit (winter water)	300 mmol NO_3^- m^{-2}	223 to 235 mg C m^{-2} day^{-1}
Priddle *et al.* 1998	Southern Ocean	Top predator demand		1.7 Gtonne C $year^{-1}$ / 30–40 g C m^{-2} $year^{-1}$
Priddle *et al.* 1998	Southern Ocean	Nutrient Deficit (remnant water)	10 mmol $NO_3^-m^{-3}$	1.5 Gtonne C $year^{-1}$
Alcaraz *et al.* 1998		^{14}C incorporation		179 to 1612 mg C m^{-2} day^{-1}
Hoppema *et al.*2000	Weddell Sea	TCO_2 depletion	84-740 mmol $NO_3^-m^{-2}$	100-1140 mg C m^{-2} day^{-1}
Varela *et al.* 2002	wAP	^{14}C incorporation		1.0-2.1 g C m^{-2} d^{-1}
Kim *et al.* 2016	Palmer Station		338 mmol N m^{-2}	
This study	Andvord Bay Spring 2015	Modified, from deep water	168 mmol $NO_3^-m^{-2}$	30-42 g C m^{-2} $season^{-1}$ / 103-292 mg C m^{-2} day^{-1}
This study	Andvord Bay Autumn 2016	Modified, from deep water	475 mmol $NO_3^-m^{-2}$	30-42 g C m^{-2} $season^{-1}$ /234-303 mg C m^{-2} day^{-1}
This study	Andvord Bay Spring 2015	^{14}C incorporation		300 to 3563 mg C m^{-2} day^{-1}
This study	Andvord Bay Autumn 2016	^{14}C incorporation		51 to 170 mg C m^{-2} day^{-1}

The orders of magnitude difference in ^{14}C incubation primary production estimate in December versus April mimics the difference in biomass that indicated slowing growth by mid-April. The variability in the timing of seasonal sea ice break up (and eventual removal) along the wAP, (Stammerjohn *et al.* 2008a, b; Meredith *et al.* 2017) affects the start of the growth period; this date is variable and unknown for spring 2015. When available, ice imagery can aid in this observation. Cameras installed around Andvord Bay for the FjordEco project should illuminate when sea and brash ice, as well as icebergs, came and went between December 2015 and March 2017 and provide additional information on circulation within the fjord (Sutherland *et al.* 2014). Based on average light availability, timing of ice retreat and meltwater stabilization in surface waters at similar latitude, conditions could allow for phytoplankton growth as early as beginning of October (Vernet *et al.* 2008; Kim *et al.* 2016). Taking a conservative approach, 15 October 2015 was assigned as the start to the growth season, allowing for nearly two months of production before sampling in mid-December 2015. Estimates generated from the NO_3^- and SiO_4^{2-} drawdown in the early season (up to this point) indicate that growth had occurred throughout the study area with the bulk of the growth, as indicated by increased chl-a concentration and decreased NO_3^- and PO_4^{3-} concentrations in the middle-fjord, associated with meltwater, as indicated by depleted surface $\delta^{18}O$, salinity, and increased temperature. There was considerably less SiO_4^{2-} drawdown compared to NO_3^- indicating this early season growth was not dominated by diatoms but rather by flagellates, mainly cryptomonads. The second period of growth, from December 2015 to April 2016, was characterized by increased NO_3^-, PO_4^{3-}, and SiO_4^{2-} drawdown within Andvord

Bay in the expanding warm, fresh, and stable surface layer. The shift in depletion ratio of Si: NO_3^- from spring to autumn (Figure 8A and 8C, respectively) suggests that diatom growth was a contributor to primary production within Andvord Bay in summer and autumn. In association with the second growth period, primary production from diatoms, per SiO_4^{2-} drawdown, accounted for 25-68% of estimated new production in Andvord Bay with the largest proportion in the middle of the Fjord (Table 3).

The premise of this method, pioneered by Jennings (1984) and still used today (Priddle *et al.* 1994; Serebrennikova and Fanning 2004; Bergeron and Trembley 2014), is having a baseline nutrient concentration upon which to calculate the drawdown, typically a 'winter water' characterized by winter sampling. Alternatively, a predicted winter mixed layer concentration can be inferred when a temperature minimum is still apparent below the summer mixed layer in (Priddle *et al.* 1996). Andvord Bay, having different dynamics than the Weddell Sea and other high latitude regions where this approach has been utilized required an alternate to true winter water. No *in-situ* measurements during the winter were made and no remnant winter water characteristics were observed during the spring or autumn. To overcome this problem, source water masses in the Gerlache Strait were identified and assumed to mix and characterize the mid- and deep-water in Andvord Bay which in turn supply nutrients to the surface water in the fjord.

Estimating primary production from nutrient deficits is advantageous because it provides an integrated result that is independent of biomass at the time of sampling and it compensates for the variation (ups and downs) of production over the span of

the growth season. Additionally, Gordon et al (2000) identified a lag in surface water replenishment and the return of cold, winter conditions in April in the Ross Sea. The summer maximum drawdown was still apparent and this delay is another reason this method seems best for seasonal or longer-term estimates of production compared to the more common methods of estimating primary production. Intense short periods of growth may be a large component of the total annual production in the fjord and these can be challenging to direct sampling. Our field sampling was constrained to spring and autumn, but a moored benthic time-lapse camera left between cruises indicated a significant export event in early January 2016 in the middle-fjord indicative of an intense bloom (CR Smith, pers. comm.). This export was observed after the mid-season replenishment of mid-December 2015 (Figure 7) followed by a several weeks of quiescence (Figure 5C). Additionally, this method may provide a seasonal estimation of primary production with only one to two annual field samplings depending on the consistency of growth period and source of nutrients to the region.

In Andvord Bay, estimating primary production from surface NO^{3-} depletion, relative to deep water concentrations, integrated over the summer growth season agrees with another seasonal estimation of primary production, the phytoplankton flux deposited in the benthos. The anomaly of accumulated chl-a in surface sediments between December 2015 and April 2016, corresponding with the second growth period, also shows the maximum sedimentation, a proxy for production, in the inner-fjord (Figure 11). Varela et al (2002) method of using surface chl-a as an estimator of primary productivity in the water column, would have indicated greater production in

Andvord Bay than outside the fjord, same as our estimates but it would not have concluded the greatest primary productivity within the inner-fjord.

The proportion of primary production associated with siliceous growth (diatoms) was also estimated and indicated little diatom growth. These estimates had further limitation within Andvord Bay because of the unique structure of silica profiles, contrast between the source water concentrations, and lack of significant surface deficit, relative to deep water, as of the spring sampling. This necessitated the change in procedure and limited these calculations to the second growth period.

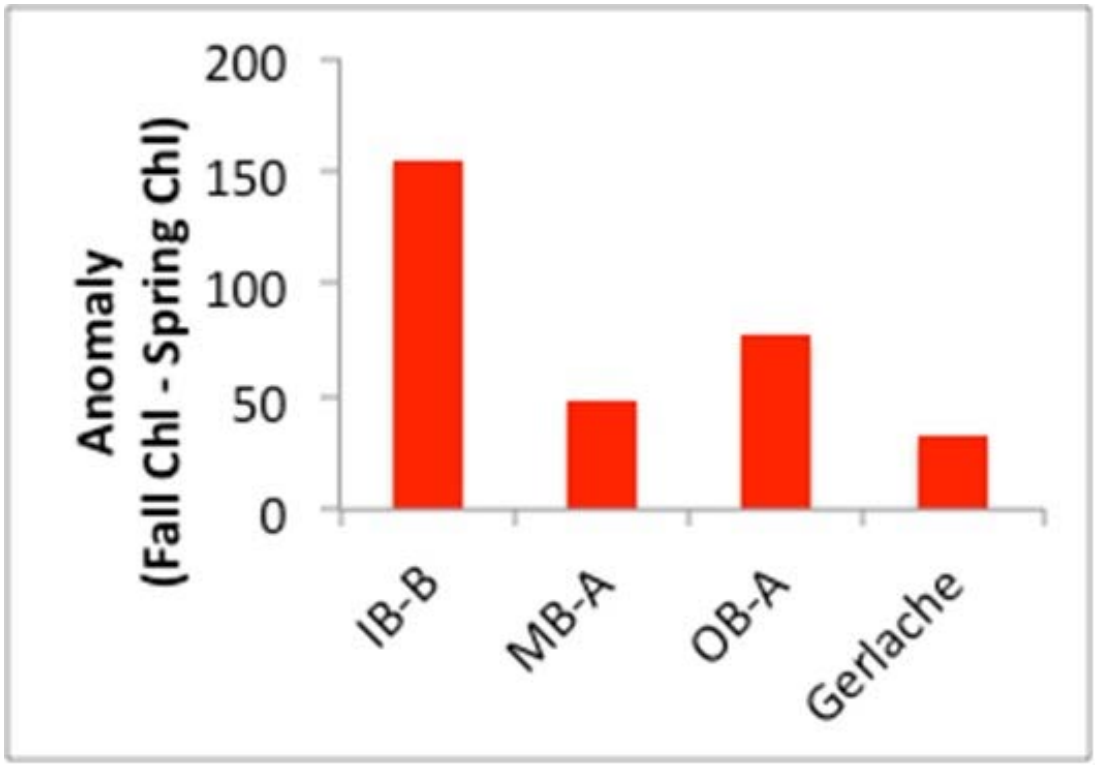

Figure 11: Sediment pigment anomaly: Surface layer (0-10 cm) sediment chl-a anomaly representative of accumulation between the sampling in December 2015 and April 2016. IB-B represents inner bay near Moser glacier, MB-A is located 13 km from glaciers, OB-A is at the fjord mouth and Gerlache is Gerlache Strait sediments.

This nutrient drawdown method inherently yields a conservative estimate or minimum expected primary production by accounting for only new production, excluding NH_4^+ and NO_2^- as N sources. The high concentration of NO_3^- and minimal presence of reduced nitrogen species in spring suggests the early season is primarily new production. In autumn, the surface NH_4^+ concentrations, nearly 4 µM, is more than sufficient to support recycled production. Goeyens *et al.* (1995) found NO_3^- drawdown to underestimate production when NH_4^+ exceeds 1.7% of total inorganic nitrogen pool. In autumn, the inner fjord NH_4^- concentration represented more than 10% of the dissolved inorganic nitrogen pool. The primary production estimate from NO_3^- drawdown also does not account for partial (1-3 µM) replenishments that may occur with occasional minor wind events, turbulent mixing, or diffusion through the nutricline. As a calculation of net community production, the method is unable to distinguish between phytoplankton and bacterial nutrient uptake. In spite of its limitations, the method employed in this study provides a good approximation for flux to the benthos as new production has been defined as equivalent to export (Eppley and Peterson 1979). In contrast, the ^{14}C incubation method yields a net primary production rate that accounts for losses by respiration that may occur over the 24-h incubation.

Physical Drivers:

In cold, high latitude, seasonally light-dependent regions, stable surface layers are important for the growth of phytoplankton. Meltwater stabilized water columns can provide the surface layer necessary for periods of high primary productivity (Laventer 1996). Smith *et al.* (2001) showed correlation between fresh water lens stability and primary production, and diatoms have been shown to dominate in well-

stratified conditions (Arrigo *et al.* 1999). On both spring and autumn in Andvord Bay, increased chl-a and the greatest nutrient deficits were associated with salinity minima. The presence of icebergs, brash ice, and sea ice may provide stabilizing freshwater with seasonal and inter-annual variability.

The geographic and hydrographic boundary layers of the fjord shields Andvord Bay from the strong currents and winds of the Gerlache Strait; they also contribute to the maintenance of a stratified water column. Strong wind events as depicted in Figure 6 illustrate how, in addition to replenishing nutrients, the loss of stratification decreases the biomass in the surface layer. With prolonged along fjord winds, biomass can be advected from the fjord or mixed below the euphotic zone, effectively resetting the system. If this occurs with certain frequency, it can lead to increased growth by simulating a semi-continuous culture.

How phytoplankton respond to transitory mixing events or shifts in mixed layer depth had been suggested as dependent on light and Fe availability (Fauchereau *et al.* 2011). Fjord systems such as the Arctic Kongsfjorden–Krossfjorden have circulation that is driven by tides, run-off, and prevailing katabatic winds (Svendsen *et al.* 2002). There has been no indication that tides or meltwater play a significant role in the circulation of Andvord Bay. Wind pulses however, coincided with reversals in subsurface flow (Figure 7) and may be the primary driver of water circulation. In a narrow fjord of this size, it is possible that any extended physical forcing will increase the typical flow in and out until diminished by friction.

Repetitive sampling before and after a prolonged wind event on 10-13 December 2015 gave us the opportunity to estimate phytoplankton population before

and after the replenishment. The wind event provided a full replenishment to surface NO_3^- concentration in conjunction with a loss of stratification. The sustained winds generated elevated wind stress for approximately 3 days (> 0.2 N/m^2 for > 24 hours; max > 0.75 N/m^2), from this an operational threshold can be defined as a wind stress greater than 0.1 N/m^2 for more than 48 hours. To assess whether this was anomalous or a frequent occurrence the threshold was applied to the Neko Harbor AWS data from 19 December 2015 through 31 May 2016, in search of additional events that could alter the stratification and mix nutrients into the surface layer. No additional wind events were recorded during the 2015-2016 season.

Identifying events capable of full replenishment was critical to applying the drawdown estimation method in order to establish a clear growth period. In turn, establishing this growth season affects the calculation of the daily rate of production. The AWS and shipboard data yielded comparable wind stress values with similar magnitude peaks at aligned times (Figure 5). The late March 2016 peaks of wind, although of similar magnitude as the December event, lack the duration and change in density profiles recorded after the December 10-13 storm (data not shown), suggesting that the duration of the event may be more important than the magnitude. These short wind events may be capable of minor replenishments on the order of a few μM, but do not appear to reset the surface layer with deep-water nutrient concentrations. The pulse addition of macro nutrients may be beneficial for growth, but would also be unaccounted for with the drawdown estimation. Furthermore, significant water property changes were observed in response to wind pulses occurring on the shelf outside Sermilik Fjord over short timescales (Jackson *et al.* 2014). Therefore, the

stronger winds and currents in the Gerlache Strait may influence circulation—and thus the success of primary production—in Andvord Bay, a physical driver unresolved by this analysis.

Conclusions:

NO_3^- and SiO_4^{2-} deficits stochiometrically converted to integrated primary production estimates were critiqued and compared to isotopic ^{14}C incubation rates as well as regional data. The quiescent Andvord Bay, with minimal currents, tidal influence, and glacial meltwater, does have occasional influential pulses of energy from strong wind events such as the one observed in mid-December 2015 which can split phytoplankton growth into two or more periods. An integrated understanding of primary production within highly variable productive region like this fjord produces estimates that represent a minimum seasonal capacity for new production better than individual, snapshot measurements that over- or under-estimate production when extrapolated. This approach to assessing the primary productivity in Andvord Bay was tested and found useful with the in-situ sampling occurring in spring and fall, bracketing the 2015-16 growth season of focus in the FjordEco project. Using biological characteristics (macronutrients and chl-a) as tracers for physical processes related to phytoplankton population dynamics resulted in a first-pass assessment of this complex system. This characterization of nutrient distribution in Andvord Bay lays the framework for further assessment of the phytoplankton community and physical-biological interactions.

The assumptions associated with utilizing nutrient drawdown were addressed in the following ways. The unknown variability of identifiable water masses as source

water in the Gerlache Strait supplying the fjord required that only data collected and analyzed during the 2015-2016 season from this region were used to assess the effectiveness of this modified method. Advection is assumed to be minimal, with average currents less than 10 cm/s in Andvord Bay, as are vertical turbulence and tides (Ø. Lundesgaard, pers. comm.). Realistic depletion time frames were determined from work at similar latitude and may be improved with ice image analysis. The repeatability of this modified method requires characterization of source water masses in the Gerlache Strait, duration of katabatic along-fjord wind events, and the timing of removal of ice from the fjord, each of which vary interannually on scales that may be affected by continued warming on the wAP.

This thesis in part is currently being prepared for submission for publication of the material. Ekern, Lindsey; Pan, Boyang; Cape, Mattias; Vernet, Maria. The thesis author was the primary investigator and author of this material.

REFERENCES

Annett, A. L., M. Skiba, S. F. Henley, H. J. Venables, M. P. Meredith, P. J. Statham, and R. S. Ganeshram. (2015). Comparative roles of upwelling and glacial iron sources in Ryder Bay, coastal western Antarctic Peninsula. Mar. Chem. 176: 21–33. doi:10.1016/j.marchem.2015.06.017

Ardelan, M. V., O. Holm-Hansen, C. D. Hewes, Reiss, C. S., Silva, N. S., Dulaiova, H., ... & Sakshaug, E. (2010). Natural iron enrichment around the Antarctic Peninsula in the Southern Ocean. Biogeosciences, 7(1), 11-25.

Arrigo, K. R., D. Robinson, D. Worthen, R. Dunbar, G. DiTullio, M. VanWoert, M. P. Lizotte. (1999). Phytoplankton community structure and the drawdown of nutrients and CO2 in the Southern Ocean. Science 283, 365–367.

Arrigo K.R., G.R. DiTullio, R.B. Dunbar, D.H. Robinson, M. Van Woert, D.L. Worthen, M.P. Lizotte (2000) Phytoplankton taxonomic variability in nutrient utilization and primary production in the Ross Sea. J. Geophys. Res., 105, pp. 8827–8845

Arrigo, K. R., G. L. van Dijken, and A. L. Strong (2015). Environmental controls of marine productivity hot spots around Antarctica, J. Geophys. Res. Oceans, 120, 5545–5565, doi:10.1002/2015JC010888.

Behrenfeld, M. J., and P. G. Falkowski. (1997). Photosynthetic rates derived from satellite based chlorophyll concentration. Limnology and oceanography, 42(1), 1-20.

Bergeron, M., and J.-É. Tremblay. (2014). Shifts in biological productivity inferred from nutrient drawdown in the southern Beaufort Sea (2003–2011) and northern Baffin Bay (1997–2011), Canadian Arctic, Geophys. Res. Lett., 41, 3979–3987, doi:10.1002/2014GL059649.

Bibby, T. S., M. Y. Gorbunov, K. W. Wyman, P. G. Falkowski. (2008). Photosynthetic community responses to upwelling in mesoscale eddies in the subtropical North Atlantic and Pacific Oceans. Deep Sea Research Part II: Topical Studies in Oceanography, 55(10), 1310-1320.

Brown, S. L., M. R. Landry, K. E. Selph, E. J. Yang, Y. M. Rii, Y. M., R. R. Bidigare. (2008). Diatoms in the desert: Plankton community response to a mesoscale eddy in the subtropical North Pacific. Deep Sea Research Part II: Topical Studies in Oceanography, 55(10), 1321-1333.

Brzezinski, M. A., D. M. Nelson. (1995). The annual silica cycle in the Sargasso Sea near Bermuda. Deep-Sea Research I, 42: 1215-1237

Cape, M. R., M. Vernet, M. Kahru, and G. Spreen. (2014). Polynya dynamics drive primary production in the Larsen A and B embayments following ice-shelf collapse, J. Geophys. Res. Oceans, 119, 572–594, doi:10.1002/2013JC009441.

Carrillo, C. J., and D. M. Karl. (1999). Dissolved inorganic carbon pool dynamics in northern Gerlache Strait, Antarctica. Journal of Geophysical Research: Oceans, 104(C7), 15873-15884.

Clarke, A., M. P. M. Meredith, M. I. Wallace, A. Brandon, D. N. Thomas. (2008). Seasonal and interannual variability in temperature, chlorophyll, and macronutrients in the northern Marguerite Bay, Antarctica. Deep-Sea Res. Part II, 55: 1988-2006, 10.1016/j.dsr2.2008.04.035

Cook, A. J., A. J. Fox, D. G. Vaughan, J. G. Ferrigno. (2005). Retreating glacier fronts on the Antarctic Peninsula over the past half-century. Science 308, 541. doi:10.1126/science.1104235 pmid:15845851

Cook A. J., P. R. Holland, M. P. Meredith, T. Murray, A. Luckman, and D. G. Vaughan, (2016). Ocean forcing of glacier retreat in the western Antarctic Peninsula. Science, vol. 353, no. 6296, p. 283, Jul.

Copin-Montegut, C. and G. Copin-Montegut. (1978). Stoichiometry of carbon, nitrogen, and phosphorus in marine particulate matter. Deep-Sea Res. 25, 911-931.

Dore, J. E., and D. M. Karl. (1992). RACER: Distribution of nitrite in the Gerlache Strait. Antarctic Journal US, 27, 164-166.

Ducklow, H. W., Baker, K., Martinson, D. G., Quetin, L. B., Ross, R. M., Smith, R. C., Vernet, M., & Fraser, W. (2007). Marine pelagic ecosystems: the west Antarctic Peninsula. Philosophical Transactions of the Royal Society of London B: Biological Sciences, 362(1477), 67-94.

Eppley, R. W. and B. J. Peterson. (1979). Particulate organic matter flux and planktonic new production in the deep ocean Nature 282, 677–680.

Epstein, S. and T. Mayeda. (1953). Variations of 18O content of waters from natural sources. Geochimica et Cosmochimica Acta, 4, 213-224.

Fauchereau, N., A. Tagliabue, P. Monteiro, and L. Bopp. (2011). The response of phytoplankton biomass to transient mixiing events in the Southern Ocean, Geophys. Res. Lett., 38, L17601, doi:10.1029/2011GL04849.

Garibotti, I. A., M. Vernet, M. E. Ferrario. (2005). Annually recurrent phytoplanktonic assemblages during summer in the seasonal ice zone west of the

Antarctic Peninsula (Southern Ocean). Deep Sea Research Part I: Oceanographic Research Papers, 52(10), 1823-1841.

Gerringa, L.J.A., A.-C. Alderkamp, P. Laan, C.-E. Thuróczy, H.J.W. de Baar, M.M. Mills, G.L. van Dijken, H. van Haren, K.R. Arrigo. (2012). Iron from melting glaciers fuels the phytoplankton blooms in Amundsen Sea (Southern Ocean): Iron biogeochemistry. Deep Sea Res. Part II, 71, pp. 16–31
Goeyens, L., P. Tréguer, M. E. M. Baumann, W. Baeyens, F. Dehairs. (1995). The leading role of ammonium in the nitrogen uptake regime of Southern Ocean marginal ice zones. Journal of marine systems, 6(4), 345-361.

Gordon L. I., J. C. Jennings, A. A. Ross, J. M. Krest. (1992). A suggested protocol for continuous flow automated analysis of seawater nutrients in the WOCE hydrographic program and the Joint Global Ocean Fluxes Study. Grp. Tech Rpt 92-1, OSU College of Oceanography Descr. Chem Oc.

Gordon, L. I., L. A. Codispoti, J. C. Jennings, J. M. Morrison, F. J. Millero, C. Sweeney. (2000). Seasonal evolution of hydrographic properties in the Ross Sea, Antarctica, 1996–1997. Deep-Sea Research II, 47: 3095-3117

Grange, L. J., and C. R. Smith. (2013). Megafaunal Communities in Rapidly Warming Fjords Along the West Antarctic Peninsula: Hotspots of Abundance and Beta Diversity. PLoS ONE, 8(11): e77917. doi:10.1371/journal.pone.0077917

Hart, T. J. (1934). On the phytoplankton of the south-west Atlantic and the Bellingshausen Sea, 1929-31, Discovery Rep., VIII, 1-268.

Hoppema, M., L. Goeyens, and E. Fahrbach. (2000). Intense nutrient removal in the remote area off Larsen Ice Shelf (Weddell Sea). Polar Biol. 23: 85. doi:10.1007/s003000050012

Kim, H., S. C. Doney, R. A. Iannuzzi, M. P. Meredith, D. G. Martinson, H. W. Ducklow. (2016). Climate forcing for dynamics of dissolved inorganic nutrients at Palmer Station, Antarctica: An interdecadal (1993–2013) analysis. Journal of Geophysical Research: Biogeosciences, 121(9), 2369-2389.

Jackson R. H., F. Straneo, D. A. Sutherland. (2014). Externally forced fluctuations in ocean temperature at Greenland glaciers in non-summer months. Nat. Geosci. 7:503–8

Jennings, J. C., L. I. Gordon, D. M. Nelson. (1984). Nutrient depletion indicates high primary productivity in the Weddell Sea. Nature 309, 51–54.

Large, W. G., S. Pond. (1981). Open ocean momentum flux measurements in moderate to strong winds, J. Phys. Oceanogr., 11, 324–336.

Laubscher, R. K., R. Perissinotto, and C. D. McQuaid. (1993). Phytoplankton production and biomass at frontal zones in the Atlantic sector of the Southern Ocean. Polar Biol 13: 471. doi:10.1007/BF00233138

Lehette, P., A. Tovar-Sánchez, C. M. Duarte, S. Hernández-León. (2012). Krill excretion and its effect on primary production. Mar Ecol Prog Ser 459:29-38. https://doi.org/10.3354/meps09746

Leventer, A., E. W. Domack, S. E. Ishman, S. Brachfeld, C. E. McClennen, P. Manley. (1996). Productivity cycles of 200–300 years in the Antarctic Peninsula region: Understanding linkages among the sun, atmosphere, oceans, sea ice, and biota. Geological Society of America Bulletin 108: 1626–1644.

Lomas, M. W., and P. M. Glibert. (1999). Interactions between NH+ 4 and NO- 3 uptake and assimilation: comparison of diatoms and dinoflagellates at several growth temperatures. Marine Biology, 133(3), 541-551.

Lomas, M. W., & Glibert, P. M. (2000). Comparisons of nitrate uptake, storage, and reduction in marine diatoms and flagellates. Journal of Phycology, 36(5), 903-913.

Long M. C., R. B. Dunbar, P. D. Tortell, W. O. Smith, D. A. Mucciarone, G. R. Ditullio. (2011). Vertical structure, seasonal drawdown, and net community production in the Ross Sea, Antarctica Journal of Geophysical research, 116, p. C 10029 http://dx.doi.org/10.1029/2009JC005954

Malcolm, J. R., C. Liu, R. P. Neilson, L. Hansen, and L. Hannah. (2006). Global warming and extinctions of endemic species from biodiversity hotspots, Conservation biology : the Journal of the Society for Conservation Biology, 20(2), 538-548.

Marra, J. (2002), pp. 78-108. In: Williams, P. J. leB., Thomas, D. N., Reynolds, C. S. (Eds.), Phytoplankton Productivity:Carbon Assimilation in Marine and Freshwater Ecosystems. Blackwell, Oxford, UK

Martinson, D. G., S. E. Stammerjohn, R. A. Iannuzzi, R. C. Smith, M. Vernet. (2008). Western Antarctic Peninsula physical oceanography and spatio-temporal variability. Deep Sea Res. II 55, 1964–1987.

Martinson, D. G., and D. C. McKee. (2012). Transport of warm Upper Circumpolar Deep Water onto the western Antarctic Peninsula continental shelf. Ocean Science, 8(4), 433.

Mendes, C. R. B., V. M. Tavano, M. C. Leal, M. S. de Souza, V. Brotas, C. A. Garcia. (2013). Shifts in the dominance between diatoms and cryptophytes during three late summers in the Bransfield Strait (Antarctic Peninsula). Polar Biology, 36(4), 537-547.

Meredith, M. P., S. E. Stammerjohn, H. J. Venables, H. W Ducklow, D. G. Martinson, R. A. Iannuzzi, ... and N. E. Barrand. (2017). Changing distributions of sea ice melt and meteoric water west of the Antarctic Peninsula. Deep Sea Research Part II: Topical Studies in Oceanography, 139, 40-57.

Mouriño-Carballido, B. (2009). Eddy-driven pulses of respiration in the Sargasso Sea Deep-Sea Res. I, 56, pp. 1242-1250

Nowacek D. P., A. S. Friedlaender, P. N. Halpin, E. L. Hazen, D. W. Johnston, A. J. Read. (2011). Super-Aggregations of Krill and Humpback Whales in Wilhelmina Bay, Antarctic Peninsula. PLoS ONE 6(4): e19173. doi:10.1371/journal.pone.0019173

Pitchford, J.W. and J. Brindley. (1999). Iron limitation, grazing pressure and oceanic high-nutrient-low chlorophyll (HNLC) regions. Journal of Plankton Research, 21(3), 525-547.

Priddle, J., F. Brandini, M. Lipski, M. R. Thorley. (1994). Pattern and variability of phytoplankton biomass in the Antarctic Peninsula region: an assessment of the BIOMASS cruises. In: El-Sayed SZ (ed) Southern ocean ecology: the BIOMASS perspective. Cambridge University Press, New York, p 49 –61

Priddle, J., R. J. G. Leakey , C. J. Symon, M. J. Whitehouse, D. Robins, G. C. Cripps, E. J. Murphy, N. J. P. Owens. (1995). Nutrient cycling by Antarctic marine microbial plankton. Mar Ecol Prog Ser
116:181-198

Priddle, J., R. J. G. Leakey, S. D. Archer. (1996). Biodivers Conserv 5: 1473. https://doi.org/10.1007/BF00051988

Priddle, J., I. L. Boyd, M. J. Whitehouse, E. J. Murphy, J. P. Croxall. (1998). Estimates of Southern Ocean primary production – constraints from predator carbon demand and nutrient drawdown. J. Mar. Syst., 17, pp. 275–288

Redfield, A., B. Ketchum, F. Richards. (1963). The influence of organisms on the composition of sea water, The Sea,2M. N. Hill, 26–77, Wiley-Interscience, New York.

Robbins, J., L. D. Rosa, J. M. Allen, D. K. Mattila, E. R. Secchi, A. S. Friedlaender, P. T. Stevick, D. P. Nowacek, and D. Steel. (2011). Return movement of a humpback whale between the Antarctic Peninsula and American Samoa: a seasonal migration record, Endangered Species Research, 13(2), 117-121.

Rubin, S. I., T. Takahashi, D. W. Chipman, J. G. Goddard. (1998). Primary productivity and nutrient utilization ratios in the Pacific sector of the Southern Ocean based on seasonal changes in seawater chemistry. Deep Sea Res Part I 45:1211-1234

Sarmiento, J. L. (2013). Ocean biogeochemical dynamics. Princeton University Press.

Serebrennikova, Y. M., and K. A. Fanning. (2004). Nutrients in the Southern Ocean GLOBEC region: Variations, water circulation, and cycling, Deep Sea Res., Part II: Topical Studies in Oceanography, 51, 1981–2002, doi:10.1016/j.dsr2.2004.07.023.

Smetacek, V. (1999). Diatoms and the Ocean Carbon Cycle. Protist 150, 25–32.

Smith, C. R., F. C. De Leo, A. F. Bernardino, A. K. Sweetman, P. M. Arbizu. (2008). Abyssal food limitation, ecosystem structure and climate change. Trends in Ecology & Evolution, 23(9), 518-528.

Smith, D. A., E. E. Hofmann, J. M. Klinck, C. M. Lascara. (1999). Hydrography and circulation of the West Antarctic Peninsula Continental Shelf. Deep Sea Res., Part I, 46: 925-949

Stammerjohn, S. E., D. G. Martinson, R. C. Smith, R. A. Iannuzzi. (2008). Sea ice in the western Antarctic Peninsula region: Spatio-temporal variability from ecological and climate change perspectives. Deep Sea Research Part II: Topical Studies in Oceanography, 55(18), 2041-2058.

Stammerjohn, S. E., D. G. Martinson, R. C. Smith, X. Yuan, D. Rind. (2008). Trends in Antarctic annual sea ice retreat and advance and their relation to El Niño-Southern Oscillation and Southern Annular Mode variability. Journal of Geophysical Research: Oceans, 113(C3).

Steig, E. J., D. P. Schneider, S. D. Rutherford, M. E. Mann, J. C. Comiso, and D. T. Shindell (2009), Warming of the Antarctic ice-sheet surface since the 1957 International Geophysical Year, Nature, 457(7228), 459-462.

Sutherland, D. A., G. E. Roth, G. S. Hamilton, S. H. Mernild, L. A. Stearns, F. Straneo. (2014). Geophysical Research Letters 41 (23), 8411-8420

Svendsen, H., A. Beszczynska-Møller, J. O. Hagen, B. Lefauconnier, V. Tverberg, S. Gerland, ... and R. Azzolini. (2002). The physical environment of Kongsfjorden–Krossfjorden, an Arctic fjord system in Svalbard. Polar research, 21(1), 133-166.

Takeda, S. (1998). Influence of iron availability on nutrient consumption ratio of diatoms in oceanic waters. Nature 393, 774–777

Tremblay, J.-E., K. Simpson, J. Martin, L. Miller, Y. Gratton, D. Barber, and N. Price (2008), Vertical stability and the annual dynamics of nutrients and chlorophyll fluorescence in the coastal, southeast Beaufort Sea, J. Geophys. Res., 113, C07S90, doi:10.1029/2007JC004547.

Trivelpiece, W. Z., J. T. Hinke, A. K. Miller, C. S. Reiss, S. G. Trivelpiece, and G. M. Watters (2011), Variability in krill biomass links harvesting and climate warming to penguin population changes in Antarctica, Proceedings of the National Academy of Sciences, 108(18), 7625.

Vaillancourt, R. D., J. Marra, M. P. Seki, M. L. Parsons, and R. R. Bidigare. (2003). Impact of a cyclonic eddy on phytoplankton community structure and photosynthetic competency in the subtropical North Pacific Ocean. Deep Sea Research Part I: Oceanographic Research Papers, 50(7), 829-847.

Vernet, M., and R. C. Smith. (2007). Measuring and modeling primary production in marine pelagic ecosystems. Principles and Standards for Measuring Primary Production, 142-174.

Vernet, M., D. Martinson, R. Iannuzzi, S. Stammerjohn, W. Kozlowski, K. Sines, R. Smith, I. Garibotti. (2008). Primary production within the sea-ice zone west of the Antarctic Peninsula: I—Sea ice, summer mixed layer, and irradiance. Deep Sea Research Part II: Topical Studies in Oceanography, 55(18), 2068-2085.

Węsławski, J. M., M. A. Kendall, M. Włodarska-Kowalczuk, K. Iken, M. Kędra, J. Legezynska, and M. K. Sejr. (2011). Climate change effects on Arctic fjord and coastal - observations and predictions, Marine Biodiversity, 41, 71-85.

Wilson, D. L., W. O. Smith, D. M. Nelson. (1986). Phytoplankton bloom dynamics of the western Ross Sea ice edge—I. Primary productivity and species-specific production. Deep-Sea Res. A 33:1375–87